Volta Geli, Marc; Bonache Albacete, Jordi , dir. Field confinement devices for RFID based on SIW technologies. 2019. (1170 Màster Universitari en Enginyeria de Telecomunicació / Telecommunication Engineering)

Master’s Thesis

Master in Telecommunication Engineering

Field confinement devices for RFID based on SIW technologies

Marc Volta Geli

Supervisor: Jordi Bonache

Department of Electronic Engineering

Escola d’Enginyeria (EE)

Universitat Autònoma de Barcelona (UAB)

July 2019

El tribunal de evaluación de este Trabajo Final de Master, reunido el día ___________, ha acordado conceder la siguiente calificación:

Presidente: ______________________________

Vocal: ______________________________

Secretario: ______________________________

El abajo firmando, ***Jordi Bonache***,

Profesor de la Escuela de Ingeniería de la Universidad Autónoma de Barcelona,

CERTIFICA:

Que el trabajo al que corresponde la presente memoria ha sido realizado bajo su dirección por

Marc Volta Geli

Y para que conste firma la presente.

Jordi Bonache, director Bellaterra, ***Julio*** de ***2019***

Resum: Alguns sistemes de comunicacions, utilitzen la propagació d'ones en el espai, no obstant, també es pot transmetre informació mitjançant el confinament d'ones. Per realitzar-ho, el camp electromagnètic es limita a un volum específic mitjançant el us d'estructures buides, en las que el camp electromagnètic es conduit per la guia d'ona i limitat en les seves fronteres. Avui en dia es difícil aconseguir una distancia de confinament adequada, amb uns nivells insignificants de radiació de fuga. Com a novetat, en aquesta tesis s'ha utilitzat la tecnologia SIW, el que comporta a omplir el buit d'una guia d'ona planar amb dielèctric, aconseguint que els camps elèctrics y magnètics estiguin confinats en el interior sense pèrdues de potencia per radiació. Per transmetrà la informació a traves del camp electromagnètic s'ha creat un slot en l'estructura i gracies al disseny de transició de la guia d'ona, es pot estudiar diferents modes de propagació. S'han implementat dos prototips que treballen en la regió freqüencial RFID.

Resumen: Algunos sistemas de comunicaciones utilizan la propagación de ondas en el espacio libre, sin embargo, también se puede transmitir la información mediante la confinación de las ondas. Para ello, el campo electromagnético debe limitarse a un volumen específico mediante el uso de estructuras vacías en las cuales el campo electromagnético es conducido a lo largo de la guía y limitado en sus fronteras. Hoy en día es difícil lograr una distancia de confinamiento adecuada, con niveles insignificantes de radiación de fuga. Como novedad, en este trabajo se ha utilizado tecnología SIW, lo que conlleva a rellenar el vacío de una guía de onda planar con dieléctrico, consiguiendo que los campos eléctricos y magnéticos queden confinados en su interior sin perdidas de potencia por radiación. Para transmitir la información a través del campo electromagnético se ha creado un slot en la estructura y gracias al diseño de transición de la guía de onda podemos estudiar diferentes modos de propagación. Se han implementado dos prototipos que trabajan en la región de frecuencias RFID.

Summary: Some communications systems use wave propagation in free space, however, information can also be transmitted by confining the waves. For this, the electromagnetic field must be limited to a specific volume through the use of empty structures in which the electromagnetic field is conducted along the guide and limited at its borders. Nowadays it is difficult to achieve an adequate confinement distance with negligible levels of leakage radiation. As a novelty, SIW technology has been used in this work, which leads to fill the vacuum of a planar wave guide with dielectric, achieving that the electric and magnetic fields are confined in its interior without loss of power by radiation. In order to transmit the information through the electromagnetic field a slot has been created in the structure and thanks to the transition design of the waveguide we can study different modes of propagation. Two prototype have been implemented that work in the RFID frequency region.

OUTLINE

LIST OF FIGURES

LIST OF TABLES

1.Introduction

Many technologies are based on object identification. Wireless components and systems have received increased interest in recent years, as new applications for millimetre waves are being introduced and developed. To this end, radio frequency identification (RFID) in the ultra-high frequency (UHF) band, with the main objective of identifying objects at longs distances. This work will focus on the use of this technology but for detection in the near field by means of a radio signal for applications such as points of sale in stores or department store.

To do this, these objects must be equipped with an RFID tag that consists of an antenna, usually a dipole that allows communication with the reader, and an integrated circuit that stores the information and therefore identifies the object.

The power supply to the data-carrying device and the data exchange between the data-carrying device and the reader are achieved without the use of galvanic contacts, using instead electromagnetic fields.

Most of the communications systems use wave propagation in free space, however information can also be transmitted by confining the waves in cables or waveguides. In this latter case it is possible to control the coverage region where the communication can be achieved.

Waveguides are structures of a conductive material of circular, rectangular or elliptical sections, in which the direction of the electromagnetic energy is guided through the line and limited in its walls. These conductive walls confine the electromagnetic field in the structure, which can be empty or filled by dielectric, so that there are no radiation losses.

The most common waveguides have rectangular cross-sections, these waveguides are formed by adding to the two parallel planes horizontal conductors two parallel planes vertical conductors, with the purpose of confining the electromagnetic energy and to serve as support to the two parallel planes horizontal conductors that help the propagation.

Substrate integrated waveguide technology (SIW) has been recently investigated for its significant advantages such as low cost, low loss, and easy integration with planar circuits. It consists of a wide microstrip line that is shorted at the edges with conductive vias, acting as a rectangular waveguide. Using SIW, rectangular waveguide based non-planar circuits can be synthesized into planar form with a dielectric substrate having two parallel arrays of via-holes analogous to waveguide metallic side walls.

Specific readers that works in the frequency of operation of UHF-RFID near the GHz range 915 MHz in USA and 867 MHz in Europe, must be designed to detect the tags within the reading distance and ignoring those that remain outside this region.

In this thesis is presented a method for generate an electromagnetic wave with controllable confinement using a structure designed with a substrate integrated waveguide technology in order to detect tags. The main objective of identifying objects at small and controllable distances from the reader. For feeding the structure, it has been designed a transition based in microstrip technology in order to obtain two different propagation modes.

1.1 Problem Statement

Actually, the readers of RFID are composed of an antenna, an RF electronic module for communicate with the tag. In these systems, the reader transmits a modulated signal with periods of un-modulated carrier, which is received by the tag antenna. The control of electromagnetic field distribution in space is of fundamental importance, because nowadays it is only possible to reduce the power density of the antenna to decrease the area of the electromagnetic fields and using conventional structures due to the presence of energy leakage in form of radiation.

To solve it, we present a method of electromagnetic field confinement based o SIW technology. With this method, the confinement volume can be controlled and two different prototypes have been implemented to ensure the RFID tag detection.

1.2 State of art

Because an electromagnetic confinement structure will be designed to work at RFID frequencies, this topic is relatively new and there is no state of the art possible. What we will see in this section is how RIFD technology currently works.

Due to the numerous advantages of RFID systems compared with other identification systems, RFID systems are now beginning to conquer new mass markets.

Radio frequency identification technology provides the capability of wireless identification and tracking capability. It is possible track objects in the warehouse, supply chain, control system, and automation process [1].

This system is characterized by the use of simple devices on one end, called tags, and on the other end of the link is found complex devices called readers. The figure 1 shows schematic of RFID system. The tags consist of an antenna and an integrated circuit chip which contain a memory, these tags can be powered by a battery called active tags, or by the radio signal sent by the reader, called passive tags. The readers are composed of an antenna, an RF electronic module for communicate with the tag, and a control electronic module, which is responsible for communicating with controller.

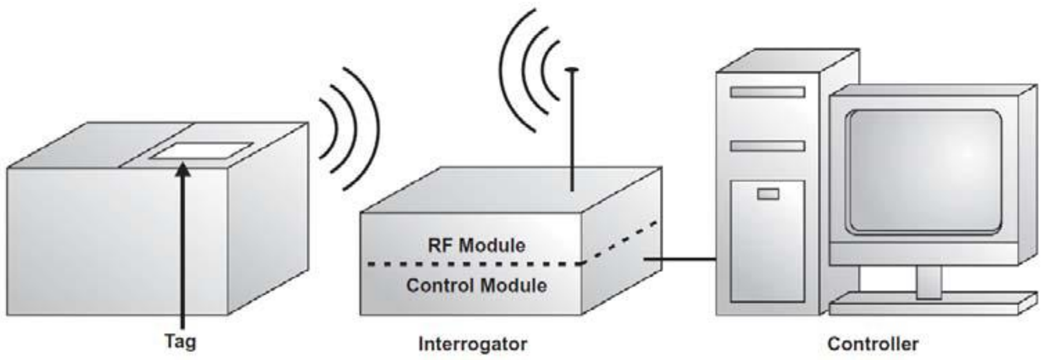

Figure 1. The basic building blocks of an RFID system

RFID system normally is used to automatic identification and data capture in order to control the stock, but for this purpose the system very well-know is the barcode [2]. Table 1 compare the principle characteristics between these systems.

	Barcode	**RFID**
Data Transmission	Optical	Electromagnetic
Data size	3 KB	64 KB (passive tags) 120 kB (active tags)
Tag Writable	No	Possible
Read Range	Several cm	15 m (passive tags) 100 m (active tags)
Security	Low	High
Environmental Susceptibility	Dirt	Low
Multiple reading	Not possible	Possible
Price	< 0.01 €	From 0.1 € (passive tag) From 10€ to 100€ (active tags)

Table 1.Comparison of barcode vs. RFID system characteristics

The great disadvantage of the RFID system is the cost, but it is believed that someday RFID tags will be as pervasive as barcodes.

Generally, the RFID systems at low frequency (LF, 125 – 134 kHz) and high frequency (HF, 13.56 MHz) bands are based on inductive coupling to carry power transfer and data transmission between the reader antenna and the tag while the RFID systems at ultra-high frequency, typically 840 – 960 MHz and microwave 2.4 and 5.8 GHz bands are based on the propagation of electromagnetic waves to transfer information between the reader and tags [3].

This thesis focus the UHF-RFID passive systems. In these systems, the reader transmits a modulated signal with periods of un-modulated carrier, which is received by the tag antenna. The chip convert the un-modulated signal to DC and sends back its information. Figure 2 shows the operation of a typical UHF-RFID system.

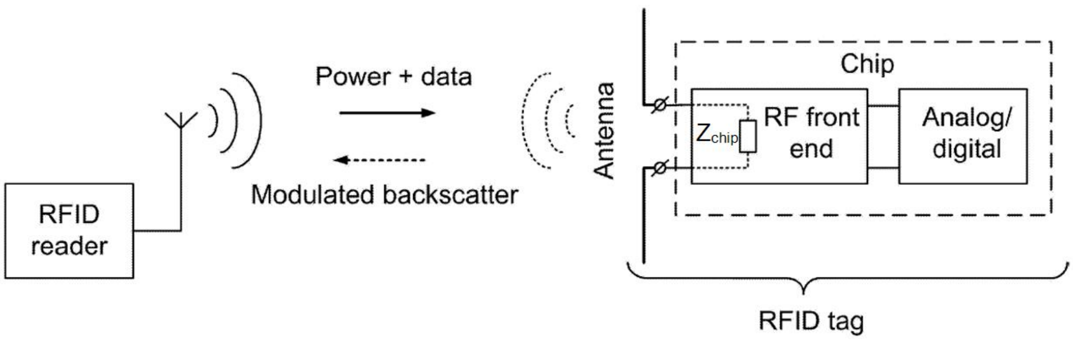

Figure 2. Operating principle of a typical UHF-RFID system

The current regulations for RFID impose the maximum level of the power density sent by the reader, whereas there is no restriction on the field polarization, which could be defined depending on the application. These two parameters, in addition to the distance between tag and reader and the characteristics of the tag antenna, determine the total power received by the integrated circuit of the tag, and hence, the maximum reading distance at which a reader can read information from the tag.

1.3 Methodology

This paper presents the design of an SIW to microstrip transition in order to create a control method of electromagnetic field confinement at the RFID-UHF band.

First there will be an introduction about the propagation of waves and the different modes that exist. As will be seen below, depending on the propagation mode, we can offer more reading area for the activation of the RFID tag. This will require designing two rectangular waveguides based on SIW technology, but each depending on the mode of propagation feeding one way or another.

For the design of the electromagnetic confinement structure, we will use Computer simulator technology (CST Microwave Studio), a software belonging to Dassault Systems. CST offer accurate, efficient computational solutions for electromagnetic design and analysis. This software will allow us to study the confined electromagnetic field and simulate the propagation distance of the electric field.

For the design of the power supply of the waveguide structure, it is necessary to create two transitions between the SIW confinement device and the Microstrip transmission lines. ADS (Advanced Design System), a software belonging to Keysight, has been used to study the different simulations. ADS is an electromagnetic simulation program, which allows both the design and simulation of circuits, as well as the design and evaluation of layout through its Momentum tool.

The effect of the transitions line length is observed on circuit performance. The following substrate has been chosen, Rogers's 3010 having relative permittivity of 11.2, loss tangent 0.0022 and 1.27 mm thickness inches.

Finally, the two devices have been manufactured and the measurements of the of the scattering parameters were obtained by means of the Agilent PNA N5221A network analyser. The comparison has been made between the actual measurements and the simulated measurements.

1.4 Outline of the Document

The remaining paper is organized as follows. In section II there is a study of the basic theory of waveguides, from how the lines of transmissions and waveguides work, the different structures of confinement that exist, the different types of propagation and finally how SIW technology works.

In section III the theoretical design of the waveguide and its simulated results are developed. In this section, you will see how the waveguide should work, the different calculations to find the dimensions of the structure, the different simulations made with the different software used.

Theme IV explains the manufacturing process and the simulations obtained from the prototypes and finally a comparison of the results of the simulations against the results of the prototypes.

The work is finally concluded in section V, this chapter describes the main conclusions explaining advantages and limitations related to this technology, and the future work derived from this master thesis.

2. Fundamental Principles

The aim of this chapter is to provide a general overview of the waveguides and its different propagations modes. All this theoretical background will be explained in detail. Firs of all it is introduced the concept of waveguides and, afterwards, the different propagation modes.

2.1 Transmission Lines and Waveguides

Transmission lines are dual conductor lines that act as transverse electromagnetic mode (TEM) wave guides for electromagnetic waves. Two-port circuit used to connect a generator or transmitter signal to a receiving load over a distance.

Some telecommunications systems use the propagation of waves in free space, however, information can also be transmitted by confining the waves in cables or structures waveguides.

Waveguides are structures of a conductive material of different sections shapes like circular or rectangular sections, in which the direction of the electromagnetic energy is guided through the line and limited in its walls. The waveguide can be filled with vacuum, air or some dielectric with permeability (μ) and permittivity (Ɛ) parameters. The wave propagates through the dielectric and is reflected by the conductive material that acts as a wall. If the conductive wall is very thin, little power is dissipated since little current flows in the conductive wall. The wave as it advances is losing amplitude due to the dielectric losses.

In the guides, electric fields and magnetic fields are confined in the space that is inside. The intensity of the fields is maximum in the centre along the length of the structure and decreases to zero when arriving at the walls.

Thanks to this propagation, it possible transmit the electromagnetic energy from one region to another region, and can carry or transmit power or communication signals. It is capable of directing power to where is needed.

Most energy above a certain frequency called cut-off frequency will pass through the waveguide, whereas most of the energy that is below the cut-off frequency will be attenuated by the waveguide. The physical dimensions of a waveguide determine the cut-off frequency for each mode.

2.2 Waveguide Structures

Since energy is transported by electromagnetic waves, the characteristics of waveguides such as impedance, power and attenuation are expressed by electric and magnetic fields characteristic of the guide under consideration. This structures can have different shapes, the most common is a rectangular shape, but it is possible found others like circular cross-section.

For this reason in the next section shown the principle characterises of each shape.

2.2.1 Circular waveguides

These circular waveguides, also called cylindrical, are those that maintain a uniform circular cross section along their length, therefore, is a flexible duct of a few centimetres in diameter, which can propagate without excessive reflections. They are used for systems where low attenuation is critical or where multiband capability is needed. They are manufactured simpler than rectangular, and their connections are easier to make, but this type of guide has more area than the rectangular that operates on the same frequency. Their applications are quite specific as radars and terrestrial microwaves.

Figure 3. Circular Waveguide Structure

2.2.2 Rectangular Waveguide

The most common waveguides have rectangular cross-sections, these waveguides are formed by adding to the two parallel planes horizontal conductors two parallel planes vertical conductors, with the purpose of confining the electromagnetic energy. Their physical dimensions are regulated by the frequency in such a way that the electromagnetic wave propagates inside the waveguide.

They are easy to manufacture and have several advantages since they have a large bandwidth and have few losses.

They are commonly used for power transmission at microwave frequencies in applications as radio frequency systems, millimetre wave systems, and in some precessions test applications.

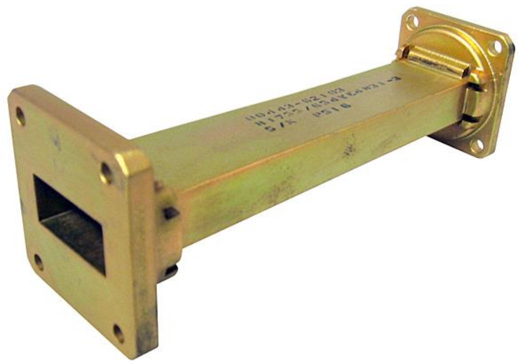

Figure 4. Rectangular Waveguide Structure

2.3 Propagation theory

In the guides, electric fields and magnetic fields are confined in the space that is inside, then in order to know how the propagation works, its necessary know how electric and magnetic fields propagates, and how the object influences them. The Maxwell equations describes that.

2.3.1 Maxwell equations

Maxwell's equations are a set of 4 equations that describe the world of electromagnetics. These equations said a flow of electric current would produce a magnetic field. If the current flow varies with time, the magnetic field will also give rise to an electric field. Maxwell's Equations shows that separated charge, positive and negative, gives rise to an electric field, and if this is varying in time as well will give rise to a propagating electric field, further giving rise to a propagating magnetic field [4]. The equation are:

- Gauss Law

$$\nabla \cdot D = \rho_V \tag{1}$$

∇ is divergence at a point (x,y,z) is the measure of the vector flow out of a surface surrounding that point. D is The Electric Flux Density is related to the Electric Field (E) and ρ_V is the electric volume charge density.

Gauss' Law says that the electric field is separated from electric charges in such a way that positive charges are a source of electric fields and negative charges act like a sink.

- Gauss Lay for Magnetism

$$\nabla \cdot B = 0 \tag{2}$$

B is the magnetic flux density.

This equation states that the magnetic field tends to wrap, how the divergence is zero the fields tend to form closed loops.

- Faraday's Law

$$\nabla \cdot E = -\frac{\partial B}{\partial t} \tag{3}$$

A magnetic field that is changing in time will give rise to a circulating E-field. So it is possible generate a E-fields from a magnetic field that is changing.

- Ampere's Law

$$\nabla \cdot H = \frac{\partial D}{\partial t} + J \tag{4}$$

Where *J* is the electric current density.

Ampere's Law says that an electric current produces a magnetic field that surrounds it. A magnetic field that is changing in time will give rise to a circulating E-field.

In order to know how the electrics and magnetics fields works, it is only necessary know that second two equations are used to numerically solve for the electrics and magnetics fields. The first two equations are not needed because they are used when all the voltage and currents are constant.

The qualitative mechanism by which Maxwell's equations give rise to propagating electromagnetic fields is represented in the figure 5.

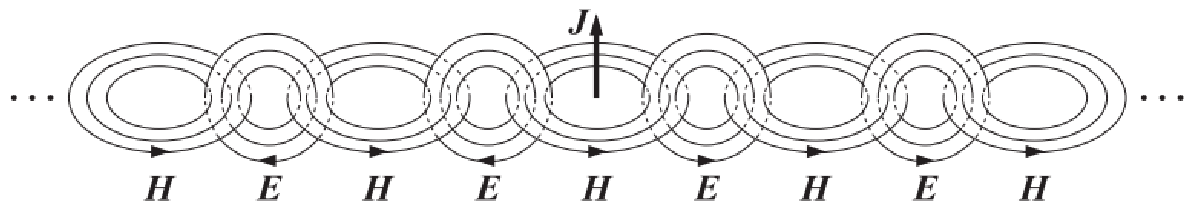

Figure 5.Propagating electromagnetic fields

A time-varying current J generates a circulating and time-varying magnetic field H, which through Faraday's law generates a circulating electric field E, which through Ampere's law generates a magnetic field, and so on. The cross-linked electric and magnetic fields propagate away from the current source. This succession produces the propagation of electromagnetic waves [5].

There are only certain configurations that the fields can assume in a waveguide. These special configurations are called modes.

Waveguide modes are time-harmonic solutions to Maxwell's equations form

$$E(x, y, z) = E(x, y)e^{-j\beta z} \tag{5}$$

$$H(x, y, z) = H(x, y)e^{-j\beta z} \tag{6}$$

where β is wavenumber.

In summary the conditions that E-field and H-field within a waveguide must meet before travels down the waveguide are:

- For an electric field to exist at the surface of the conductor, it must be perpendicular to the conductor. An electric field cannot exist parallel to a perfect conductor.
- For a varying magnetic field to exist, it must form closed loops in parallel with the conductors and be perpendicular to the electric field.

Energy travelling down a waveguide is like the electromagnetic waves travel in free space. The difference is that the energy in a waveguides is confined to the physical limits of the guide.

In the next section it is explained the different modes and specially the TE mode that is used in this thesis.

2.3.2 Propagation Modes

Each mode is described by the field profile that describes how the mode looks and the propagation constant that describes how the mode propagates through the waveguide [6].

The degenerated modes are the special case when two modes have the same propagation constant. These modes have same cut off frequency but different field configuration. This is important because the modes will remain synchronized as they propagate, which makes it very easy to couple energy from one mode to another. Thus, waveguide selection are such that higher modes are not supported in the operating band and thus only desire modes propagate through this waveguide.

A waveguide supports three modes of propagation [7], and it will be seen below.

2.3.2.1 Transverse electromagnetic modes (TEM)

In electromagnetism, a transmission line transmits the fundamental TEM mode which propagates signals at arbitrary low frequencies. This require at least two conductors, for this reason an electromagnetic TEM wave cannot be propagated within a waveguide because it only has one conductor. The TEM wave is characterized by the fact that both the electric vector, also called E vector, and the magnetic vector, also called H vector, are perpendicular to the direction of propagation. In order to clarify this concept Figure 6 an example of this propagation.

TEM wave cannot have a tangential component of the electric field on the walls of the waveguide, which is a limitation of Maxwell's equations, as a wave cannot travel directly down a waveguide without reflecting off to the sides.

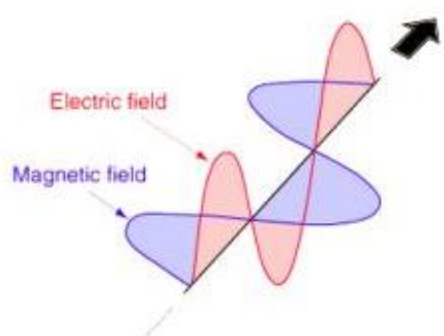

Figure 6. TEM mode

The electric field oscillates vertically in relation to the ground and respect to magnetic field vibrate at night angels to each other.

2.3.2.2 Transverse Magnetic modes (TM)

The transverse magnetic waves, called E waves, characterized by the fact that the magnetic vector is always perpendicular to the direction of propagation. Figure 7 represents this propagation.

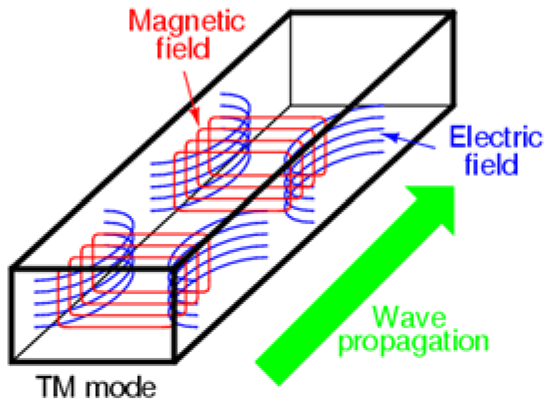

Figure 7. TM mode

The most important thing is that electric and magnetic fields are always perpendicular to each other. This is a primary principle that Maxwell discovered. The two fields always travel together in electromagnetic waves.

Where in TM modes the electric field is in the direction perpendicular to that of propagation, so only magnetic field propagates within the waveguide.

2.3.2.3 Transverse Electric modes (TE)

This waveguide mode is dependent upon the transverse electric waves, called H waves, characterized by the fact the electric vector is always perpendicular to the direction of propagation.

There is a longitudinal component of magnetic field and for this reason the TE waves, and also H.

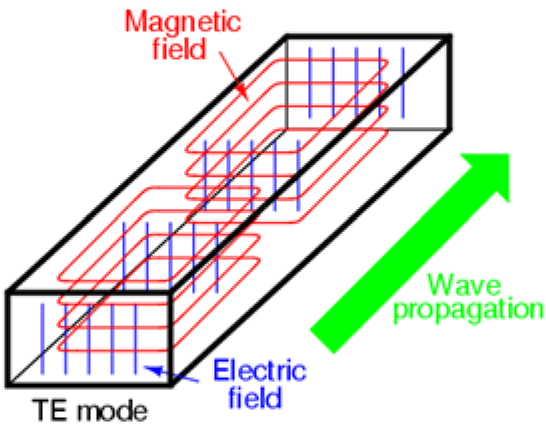

Figure 8. TE mode

As figure 8 shows, in TE modes the magnetic field is in the direction perpendicular to that of propagation, only electric field propagates within the waveguide.

In a microwave system, the analytical expressions for the electric and magnetic field must comply with the following:

- The solutions of the field components must simultaneously satisfy Maxwell's equations.
- Solutions of electric fields, such as magnetic fields, must satisfy the boundary conditions on the guide surface. Definitely, TEM has two conductors and TE or TM has at least one conductor or dielectric.

The angles of incidence and reflection depend upon the operating frequency. At high frequencies, the angles are large and therefore, the path between the opposite walls is relatively long as show in figure 9.

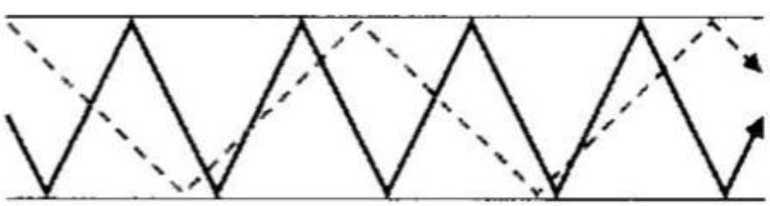

Figure 9. Wave reflection depending operation frequency

The dashed line represents a lower mode and the solid line represents a higher mode. High order modes travel greater distance, although the propagation is at the speed of light, the greater distance traveled causes the effective speed to be reduced along the guide and occurs a more dispersion effect.

When the operating frequency reaches the cutoff frequency of the waveguide, the signal simply bounces back and forth directly between the side walls of the waveguide and has no forward motion [8].

At cut off frequency and below, no energy will propagate. At cut off frequency and below, no energy will propagate.

In summary, an electromagnetic field is comprised of electric and magnetic fields which are perpendicular to each other. These fields have different patterns for each mode. These patterns depend on the mode numbers *m* and *n* and the dimensions of the waveguide. The electric field and magnetic field pattern are different for various modes in different waveguides. The electric field component of an EM wave is characterized by Ex, Ey and Ez components of the wave. Similarly, the magnetic field component of an EM wave is characterized by Hx, Hy and Hz components of the wave. The x, y and z parameters represents the Cartesian coordinates and the waveguide model is analysed on that. The waveguides extends to infinite along de z axis and the cross section is placed in the x,y plane.

The waves travel through a waveguide:

$$E(x,w,z) = E(x,y)e^{-\gamma z} \tag{7}$$

$$H(x,w,z) = H(x,y)e^{-\gamma z} \tag{8}$$

Transverse components E_x,E_y, H_x, H_y are expressed in terms of the longitudinal components E_z, H_z. These components depend on mode have expressed as that:

TE mode:

$$E_z = 0, H_z \neq 0 \tag{9}$$

TM mode:

$$E_z \neq 0, H_z = 0 \tag{10}$$

TEM mode:

$$E_z = 0, H_z = 0 \tag{11}$$

The order of the mode refers to the field configuration in the guide, and is given by *m* and *n* integer subscripts, TE_{mn} and TM_{mn}.

- The *m* subscript corresponds to the number of half wave variations on the field in *x* direction.
- The *n* subscript corresponds to the number of half wave variations on the field in *y* direction.

Notice that when *m* and *n* are equal zero, means a infinite field amplitudes, which is not a physical result. Consequently, TE or TM with these parameters equal to zero are not allowed.

This work has been designed a rectangular waveguide, for this reason before continuing with the design is recommended a few brief explanations of the behaviour of these waveguides for the mode required. Below you will see the different configurations for the TE mode of the rectangular waveguides.

Each mode has an associated cut-off frequency, so that if the frequency of the signal to be transmitted is greater than the cut-off frequency, the electromagnetic energy will be transmitted through the guide without attenuation. In another case, if the frequency of the signal is lower than the cut-off frequency, the energy will be attenuated exponentially with the distance, having a value extremely low at a very short distance this case is called evanescent wave. If more than one mode is propagating, the waveguide is said overmoded.

Dominant mode will be determined by the mode having lowest cut-off Frequency, the TE10 node is used as dominant mode in a rectangular waveguide structure. So, operating frequency must be above cut off frequency of dominant mode and below cut off frequency of next higher order mode.

The TE20 mode is the next higher order mode and it is harmonically related to the cut-off frequency of the TE10 mode. This relationship, attenuation and propagation characteristics, determine the normal operating frequency range of rectangular waveguide

It is therefore best to select the waveguide dimensions so that, for a given input signal, only the energy of the dominant mode can be transmitted by the waveguide. For example, for a given frequency, the width of a rectangular guide may be too large.

The intensity of electrics fields is represented by arrows perpendicular to the surface of the guide. The following figure represents a cross-sectional view, shows a steady-wave configuration within the guide, with the E-field varying in sinusoidal form, and takes the value of electric vector equal to zero along the walls of the guide [9].

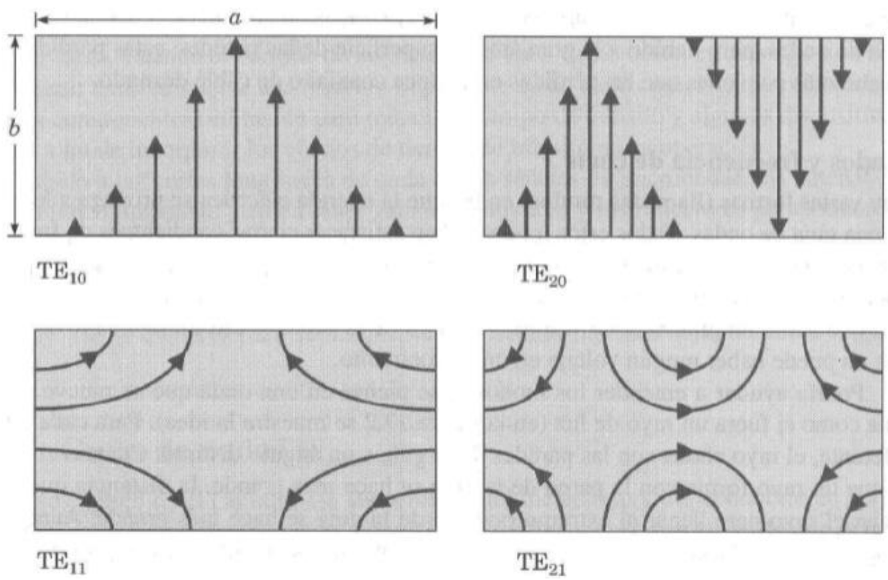

Figure 10. Stationary wave configuration inside the guide.

When the *m* parameter increase the number of wave half-cycle increases in a direction. TE_{10} mode occurs when the height equals 1/2 wavelength of the cut-off frequency, the electric field goes from 0 to max and back to 0 and TE_{20} occurs when the width equals one wavelength of the lower cut-off frequency.

When the *n* parameter increase the number of half wave variations increase in b direction.

The propagation constant inside the waveguide structure is

$$\beta = \sqrt{k_0^2 - k_C^2} = \sqrt{k_0^2 - \left(\frac{m\pi}{a}\right)^2 - \left(\frac{n\pi}{b}\right)^2} \qquad (12)$$

Where a is the width of the structure waveguide and b is the height, and k_0 corresponds to the wavenumber of the signal propagation in air.

Which is seen to be real, corresponding to a propagation mode, when

$$k_0 > k_C = \sqrt{\left(\frac{m\pi}{a}\right)^2 + \left(\frac{n\pi}{b}\right)^2} \tag{13}$$

The wavenumber in free spaces is defined as:

$$k_0^2 = \left(\omega\sqrt{\epsilon_0 \mu_0}\right)^2 \tag{14}$$

Where ω is the frequency that works, ϵ_0 is the electric permittivity in vacuum and μ_0 is the magnetic constant or the permeability of free space.

The fields in the open periodic structure vary in both the longitudinal and transverse directions.

Consequently, the propagation constants is:

$$\beta = \sqrt{\left(\omega\sqrt{\epsilon_0 \mu_0}\right)^2 - \left(\frac{m\pi}{a}\right)^2 - \left(\frac{n\pi}{b}\right)^2} \tag{15}$$

Since β always have a value equal to the wavenumber in free space minus the k_C^2, that means that the propagation constant inside the structure will be smaller than outside and the structure will radiate as figure 11 represents.

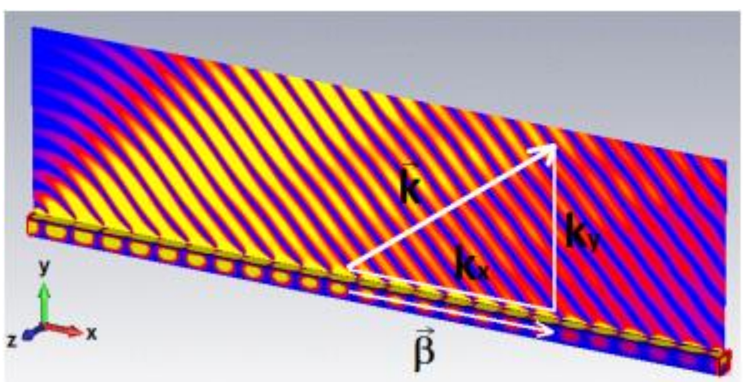

Figure 11. Field distribution, radiative mode

The components k_x and k_y correspond to the projection of the longitudinal and transverse components of k_o.

A mode is only supported above its cut-off frequency. The cut-off frequency is given by:

$$f_{c_{mn}} = \frac{k_C}{2\pi\sqrt{\mu_0\epsilon_0}} = \frac{1}{2\pi\sqrt{\mu_0\epsilon_0}}\sqrt{\left(\frac{m\pi}{a}\right)^2 + \left(\frac{n\pi}{b}\right)^2} \tag{16}$$

In order to simplify this equation for the modes that *m* parameters changes and *n* is zero, it used the next equation.

$$f_{c_{m0}} = \frac{m}{2a\sqrt{\mu_0\epsilon_0}} \tag{17}$$

Consequently, each mode has a different cut-off frequency and if the frequency of the signal to be transmitted is greater than the cut-off frequency calculated with the equation (18), the electromagnetic energy will be transmitted through the guide without attenuation.

Moreover, it is possible to observe a relationship between the cut-off frequency and the propagation mode. For a structure with fixed width, the cutting frequency increases twice as much for the TE_{20} mode respect to the TE_{10} mode. Therefore, if it is wanted to achieve a behaviour similar to the TE_{20} mode for a fixed operating frequency and fixed width, the only is to have two or more modes with the same cut-off frequency and they are said to be degenerate modes.

The figure 12 shows a het map of the electrical field intensity of different modes:

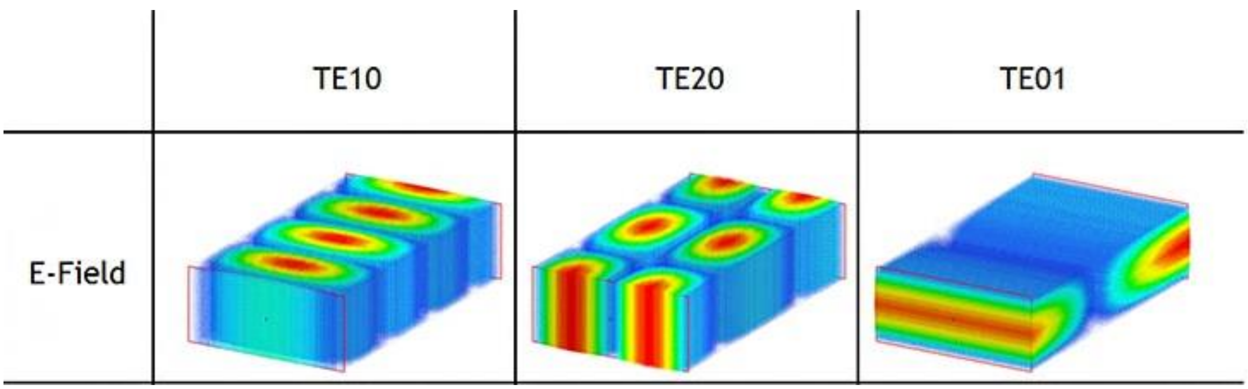

Figure 12. Distribution of electric fields in the transverse plane of different modes

This diagram is a field pattern and show the variation of electric field lines [10].

We have just done an overview of waveguides and propagation modes. Next, in the next point we will see the basics of SIW technology and what it consists of.

2.4 Substrate Integrated Waveguide technology

Various microwave waveguide components, such as couplers, detectors, isolators, phase shifters and slotted lines, are commercially available for various standard waveguide bands, and these waveguide components present properties of low loss and high power.

Because of their bulky size, their use is however limited in some of practical applications, and It is also difficult to manufacture them in mass production. With trends towards miniaturization and integration, planar transmission line structures, such as microstrip and stripline rather than waveguide, have been used in many commercial applications.

Over the past decade, SIW has developed into a mature technology and has proven to be an alternative to conventional all metal waveguides for the design of microwave millimetre waves [11].

There have been many research activities to develop new platforms of transmission lines to reduce circuit size, simplify manufacturing process, lower production cost and maintain high performance. To overcome these issues, substrate integrated waveguides have recently been proposed as alternative structures to conventional transmission lines.

SIW is a transition between microstrip and dielectric-filled waveguide (DFW). Dielectric filled waveguide is converted to substrate integrated waveguide (SIW) by the help of vias for the side walls of the waveguide [12]. These structures are fabricated by using rows of conducting cylinders or slots embedded in a dielectric substrate that electrically connect two parallel metal plates, which interrupt the current flow on the top wall.

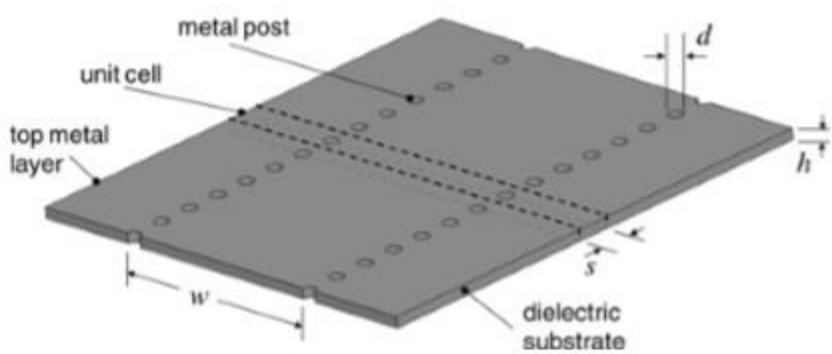

Figure 13. SIW structure

It can be easily fabricated with standard PCB process, thick-film process or LTCC process, and is easily integrated into microwave and millimetre wave integrated circuits. in order to connect active circuits to SIW or to measure S-parameters, mounting SMA connectors and microstrip-to-SIW transitions is required.

At millimetre wave frequencies and above, metal is not a god conductor, so metal waveguides can have increasing attenuation. At these wavelengths, dielectric waveguides can have lower losses than metal waveguides.

In this way, SIW structure exhibit propagation characteristics similar to the rectangular waveguides, including dispersion characteristics and field pattern, but the main difference in terms of dimensions resides in the height. In the standard rectangular waveguide the height h is usually about a half of the width, while in SIW the height is much smaller than the width and it corresponds to the thickness of the dielectric substrate, used in the PBC fabrication [13].

Because there are vias at the sidewalls, top and bottom planes are grounded, so the transverse magnetic modes do not exist and transverse electric mode exists in SIW. TE10 is used as dominant mode in SIW structure. In TE mode E field is wholly transverse to the waveguide, so E-field is perpendicular to the broad dimension of SIW.

The next table summarized the advantages and disadvantages to use this kind of technology.

Advantages	Disadvantages
• Radiation losses are lower. • Size reduction. • No bulky transitions between elements, thus reducing losses and parasitic. • Fabrication cost is lower. • Due to use of metal, conductor loss is lower. • Considerably reduce packaging, EMC/EMI, interconnect and assembly problems that are of major concern in	• Leakage losses are substantial which depends on separation of via holes placed on the top planes. • Due to use of dielectric into the waveguide structure, dielectric losses will occur compare to air used in normal rectangular waveguide. • Due to its waveguide structure, SIW exhibits cutoff frequency of lower values.

current microwave and millimeter equipment and systems.	

Table 2. Advantages and Disadvantages SIW technology

2.5. Confinement of the Electromagnetic field by means of a SIW structure

Expression (16) was obtained for the case of hollow waveguides. In case of using dielectric filled waveguides, like SIW, ϵ_0 must be placed be $\epsilon_r \cdot \epsilon_0$.

$$\beta = \sqrt{\left(\omega\sqrt{\epsilon_r \cdot \epsilon_0 \mu_0}\right)^2 - \left(\frac{m\pi}{a}\right)^2 - \left(\frac{n\pi}{b}\right)^2} \tag{18}$$

The β can be adjusted by appropriately choosing the effective dielectric permittivity (ϵ_r) of the dielectric of the SIW. Since the value of β can be adjusted in the design stage of the structure, it is possible to impose the level of confinement of the electromagnetic field around the structure. Moreover, since radiation is prevented, the dimensions of the structure might be arbitrarily large in order to increase the coverage area.

To do this the propagation constant within structure β must be larger than the propagation constant outside the structure k_0.

Therefore, choosing a dielectric with a higher effective dielectric permittivity, we will obtain that the constant of propagation inside the structure is greater than the constant of propagation outside, which leads to that a good electrical confinement is obtained, as it can be shown in figure 14, and radiation does not occur.

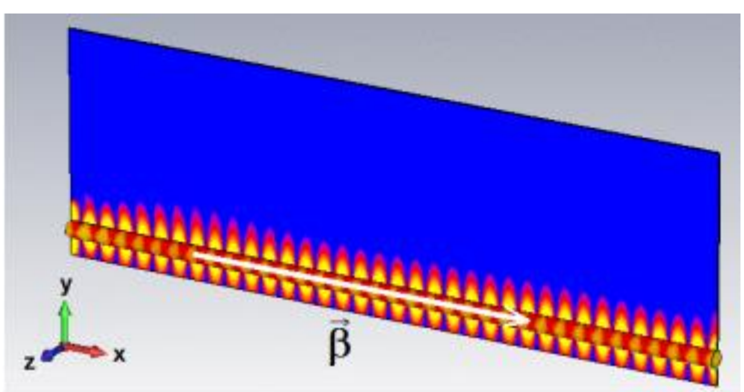

Figure 14. Field distribution, evanescent mode operation

3. Theoretical Waveguide Design and Simulation.

In this section, will be explained the steps followed to obtain the final design structure and the measures to the simulations results. In order to calculate the simulation, the measures are optimized together, and different transitions have been designed, to calculate a low reflection in the desired operation frequency.

The proposed method consists in designing a dimensional substrate integrate waveguide structure that propagates a surface wave mode with controllable levels of field decay. For this purpose, the rectangular structure has been designed with TE propagation mode. This structure will have a slot along the z-axis the guide in order propagate de E-fields to power the tags RFID. Figure 15 is a representation of the structure that you want to design.

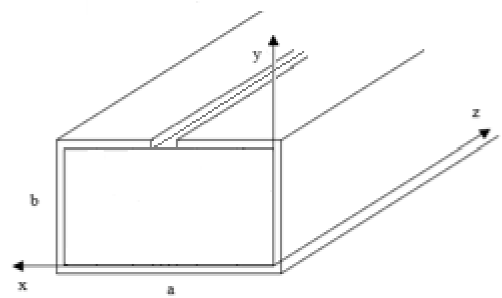

Figure 15. Conceptual design of the structure with slot

The slot is situated on the top layer, then the structure is symmetric. Also, it is possible to see the top and bottom are metal layers connected each other with the metallic vias on the sidewalls allowing to ground the layers and interrupting the current flow at the ends. This technique of connecting the layers by means of metals at the ends is cheaper and easier to manufacture than the holes that are introduced into the structure and then metallized.

The field distribution around the structure is determined by the interaction of the electromagnetic field visible the waveguide with the slot.

From the application point of view, this structure can be directly applied to an UHF-RFID nearfield reader since a zone where the tag can be detected is clearly defined. Commercial UHF-RFID tags usually need an electric field around 1 V/m for their activation.

In order to excite the RFID tag, the waveguide structure will be excited to work at different mode to increase the possibility of the tag detecting the E-fields leaving the designed electromagnetic confinement structure, because according to the mode of propagation, the electric field will be oriented in the x or y direction. However, as will be seen below, the dimensions of the electromagnetic confinement structure depend on the mode in which it is worked. For this, the structure, depends on how this designed the excitation of the structure we can work in two different modes of propagation.

In this thesis, we will work with the first two modes that appear in the structure with the slot. The modes sought are those that have a behavior similar to the dominant mode and the TE20 mode with the idea that the electric field is propagated through the slot transversely and parallel to the slot, which leads to obtain an electric field that propagates both in the direction x and y, and therefore, we get more area for the RFID tag to activate. For this reason, we will explain how is the transition of each modes.

In order to feed the structure to obtain a similar propagation of dominant mode like figure 16 show, it is necessary to create a transition that feeds the confinement structure in a symmetrical feed or common mode.

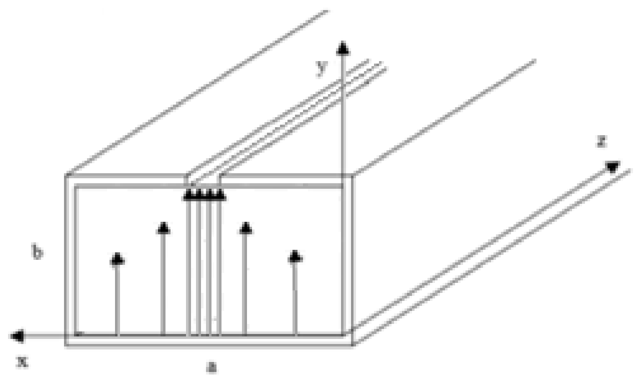

Figure 16. Dominant mode propagation

If the power supply is symmetrical, the effect of a magnetic wall just in the middle appears in the slot. This magnetic wall divides the structure in two, but the feed has the same phase, the propagation mode is very similar to the dominant mode. That is why the expected electric field is parallel to the slot.

To feed the structure to obtain a similar propagation mode like TE_{20}, it is necessary to create a transition that feeds the confinement structure in a differential feed or differential mode. When that's occurs in the middle of slot appears an electric wall which divides the structure in two parts with different electric field orientation.

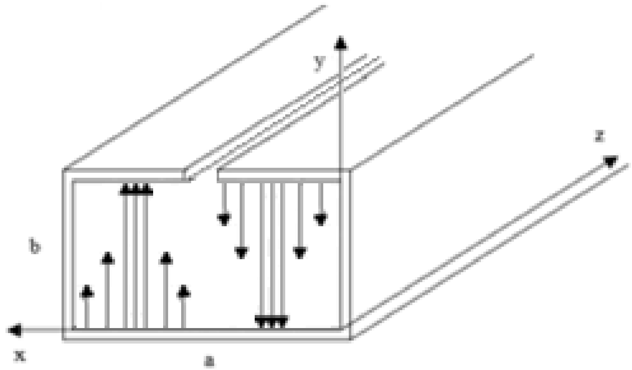

Figure 17. Degenerate mode propagation

3.1 Dimensions of the waveguide structure.

In the propagation mode of rectangular waveguides, is necessary at least a distance of a half wave length $\lambda_c/2$ across the broad dimension of the electric field, during propagation through wave-guide the electric field is perpendicular to the direction of propagation. It is equal to λ/2 across x-axis.

The guide wavelength is defined as the distance between two equal phase planes along the waveguide, and is equal to

$$\lambda_g = \frac{2\pi}{\beta} > \frac{2\pi}{k} = \lambda \tag{19}$$

Which is thus greater than λ, the wavelength of a plane wave in the filling medium. The phase velocity is:

$$\vartheta_p = \frac{\omega}{\beta} > \frac{\omega}{k} = \frac{1}{\sqrt{\mu\varepsilon}} \tag{20}$$

Which greater than $1/\sqrt{\mu\varepsilon}$, the speed of the light in the filling material. In addition, for TE_{10} mode,

$$k_c \approx \pi/\mathrm{a} \tag{21}$$

$$\beta = \sqrt{k^2 - (\pi/\mathrm{a})^2} \tag{22}$$

The power flow down results gives nonzero real power only when β is real, corresponding to a propagating mode.

The proposed method consists in designing a SIW guiding structure that propagates a surface wave mode with controllable levels of field decay in a surrounding medium. For this purpose, the wave number β of the guiding mode must be tailored to obtain the required exponential decay factor α_y.

$$\alpha_y = \sqrt{\beta^2 - k_0^2} \tag{23}$$

Where α_y is a positive real number. That supposes an exponential decrease of the electric and magnetic field with the distance in the broadside direction. Since the value of β can be adjusted in the design stage of the waveguide, it is possible to impose a level of confinement of the electromagnetic field around the structure.

The lower limit for α_z corresponds to a wavenumber $\beta = k_0$, whereas the upper limit is determined by the maximum achievable value for β.

The parameter $1/\alpha_y$ can be defined as a characteristic distance *d*, since it determines the maximum length where the field will be present.

In our case this attenuation distance was set to 8.7cm, or equivalently, 0.25 times the free-space wavelength at 867 MHz, corresponding to an attenuation of 1dB/cm [14], and to achieve this value, the wavenumber was forced to

$$\beta = 21.4569 \ {}^{rad}/_{m} \tag{24}$$

In order to calculate the width of the structure, and knowing the β value, according to equation (15) the parameters *m* and *n* have been selected according to dominant TE_{10} mode. However, the ϵ_0 parameter is the permittivity in vacuum, but in this case, is used a SIW technology, consequently inside the confinement structure there is no air, is dielectric material.

To solve the equation is necessary to know the type of dielectric material to be used.

The substrate is chosen according to the function of the application to be designed. For a low frequency application, such as this, substrates with a high dielectric constant of the order of 9 to 11 are used, as this helps to reduce the size of the circuits. Copper is chosen for the conductive material.

In this case, the dialectic material used is Rogers 3010. These laminates offer excellent stability of dielectric constant over temperature including the elimination of the step change in dielectric constant. Therefore, the main dielectric characteristics are:

- Dielectric permittivity (ε_r): 11.2
- Thickness Inches: 1.27mm
- Dissipation Factor (δ): 0,0022

Permittivity of vacuum is:

$$\varepsilon_0 = 8.85 \cdot 10^{-12}\, {}^{F}\!/_{m} \tag{25}$$

Magnetic permeability at the free space has the next value:

$$\mu_0 = 4\pi \cdot 10^{-7}\, {}^{H}\!/_{m} \tag{26}$$

Knowing that ω is the angular frequency equal to

$$\omega = 2\pi \cdot f \tag{27}$$

Thus, with all parameters found, it is possible to extract the width of the waveguide structure using the equation (16), the width of the waveguide has been calculated and it has the next value:

$$a = 56{,}75\, mm \tag{28}$$

In terms of the others dimensions the height is not a critical parameter for the design in the dominant mode. This dimension is the result of the dielectric and two conductive layers thickness.

Respect to the substrate thickness *h* is selected based on availability from manufacturers, it is equal to 1.27 mm, and the metallization thickness is equal to 0.035 mm and, consequently, the height has the next value:

$$b = 1.34\, mm \tag{29}$$

The length of the structure is maximized to the maximum that can be manufactured, thus increasing the detection area so that the tag, and being above the cut-off frequency, there is no attenuation to propagate.

As far as the size of the slot is concerned, the width should be as small as possible but allow the output of the electric field, and at the same time, do not modify the propagation mode as occurs in a closed waveguide without slot.

Once the width is known, it is possible calculate the cut-off frequency for TE_{10} mode according to equation (17), obtaining a cut-off frequency equal:

$$f_{c_{10}} = 811.2\ MHz \tag{30}$$

This implies that below this frequency there will be total reflection. Therefore operating frequency must be above cut off frequency of dominant mode and below cut off frequency of next higher order mode.

As underlined in theory chapter, the cut-off frequency between the modes is harmonically. That means that the frequency at the next higher mode is the double than dominant mode. Therefore, the operation frequency should be among those frequency, and how the operation frequency is 867 MHz this condition is met.

The table 3 represents the relation between the mode with cut-off frequency and waveguide width.

TE mode	Cut-off frequency (MHz)	Waveguide width (mm)
TE_{10}	811.2	55.227
TE_{20}	1622.4	110.454
TE_{30}	2433.6	165.681

Table 3. Cut-off frequency of different TE modes

As it has seen in the previous width calculation, in the case that it is required to work in another mode, for example TE_{20} mode, it is necessary increase the order of the parameter *m*. If this parameter increase, it implies that the width of the waveguide structure changed and that is not possible.

For this reason, a degenerate mode has been designed with the intention of being able to simulate the behavior that would be obtained if working in TE_{20} mode without the need to change the width of the confinement structure.

Once the dimensions of the waveguide has been calculated, the next step is design the structure in the CST software in order to obtain the simulations behavior.

3.2 CST Structure Design

The rectangular waveguide is modeled in CST Studio, and their field distribution analyzed. The settings are optimized for an RF waveguide component, consequently the units are set to mm and GHz.

The first step is to create the conductive layer that envelops the dielectric. This conductive layer connects the upper layer to the lower layer, so this conductor will be grounded. The conductor is set to perfectly electrical conductor (PEC) material. Figure 18 shows the conductor with the dimensions calculated in the last theme.

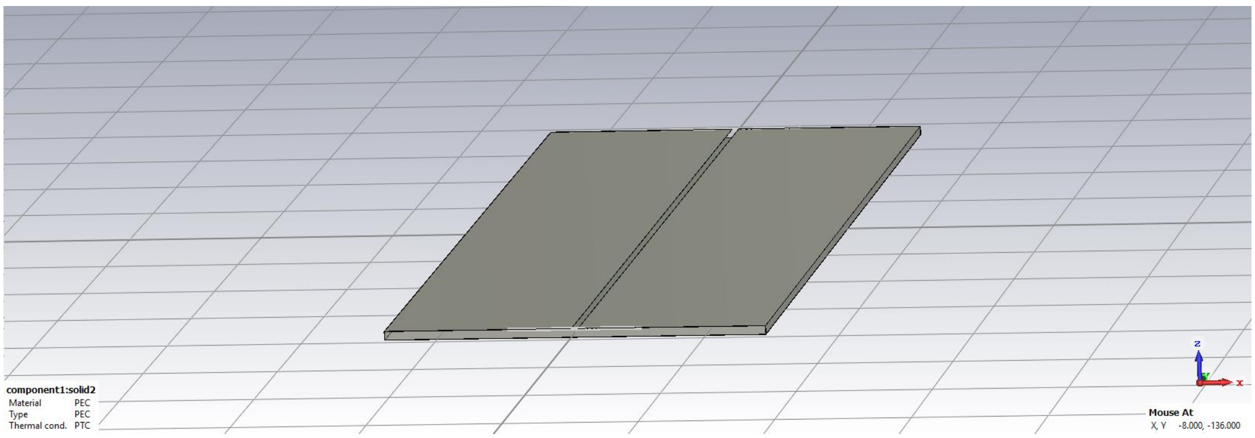

Figure 18. CST conductive structure design

As it can be seen, only the conductive structure of the waveguide has been created, therefore it is necessary to model the vacuum inside the waveguide with the chosen substrate Rogers 3010 with its parameters.

Below, figure 19 represents a front view of the structure where you can identify the measurements of the structure and are summarized in table 4.

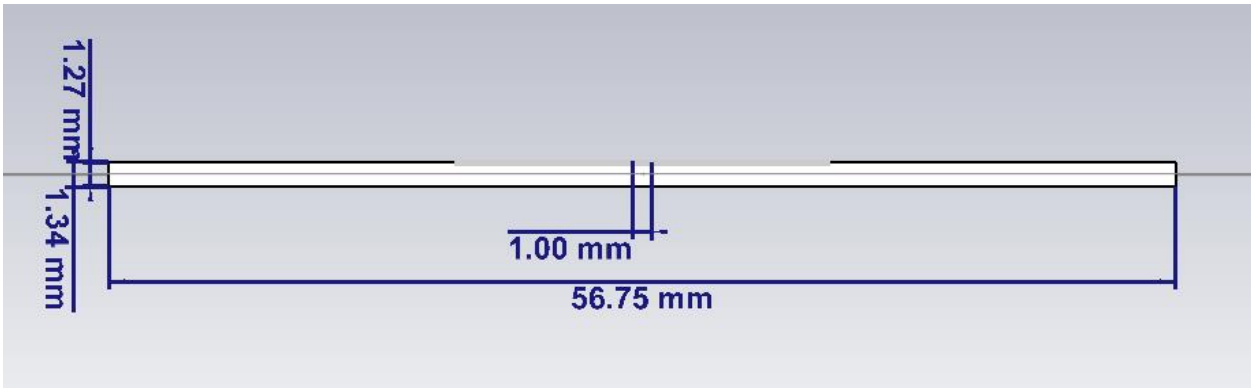

Figure 19. Dimensions of the structure

Description	Expression	Value (mm)
Structure width	a	56.75
Metallization thickness	t	0.035
Slot width	s	1
Structure height	b	1.34
Structure length	c	171

Table 4. summary of the structure dimensions

3.3 CST Structure Simulation

Once the waveguide is designed, the next step is create a waveguide port at each end of the slot. Waveguide ports represent a special kind of boundary condition of the calculation domain, enabling the stimulation as well as the absorption of energy. This kind of port simulates an infinitely long waveguide connected to the structure as show figure 20. These ports allow simulate the different modes propagation and give us the value of β and it is possible represent the E-field simulation and the magnitude.

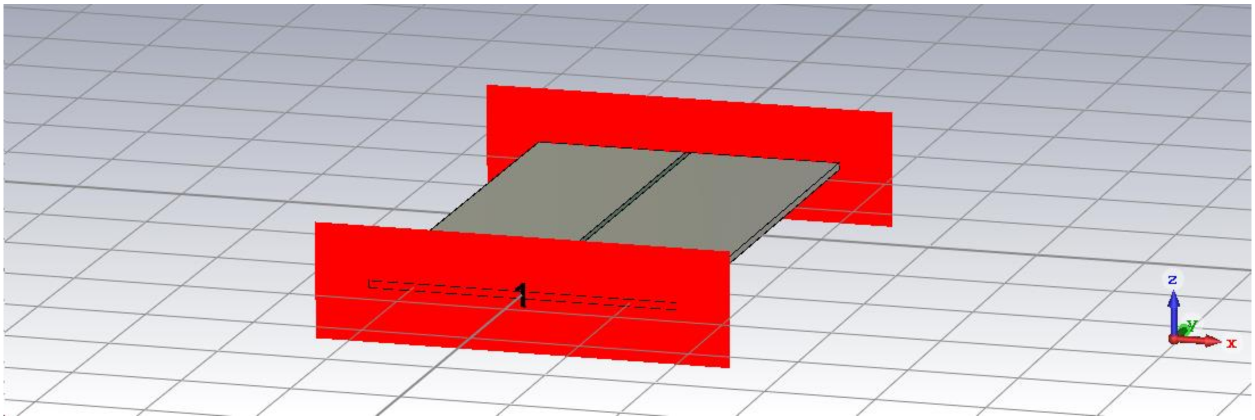

Figure 20. Structure with Waveguide Ports CST

To analyze the field distribution for different modes is carried out using the time domain solver because the boundary conditions are electric in all direction. It may be noted down that electric fields are vertically directed.

Figure 21 represents a cross-sectional view the E-field in the port in the first mode that appears and as it can be seen, it has the same behavior than the dominant mode. As it has been explained in the theory part, the electric fields are represented by arrows perpendicular to the surface of the guide with E-field varying in sinusoidal form, and goes zero from the walls of the guide to the maximum intensity in the center of the structure where the slot is located.

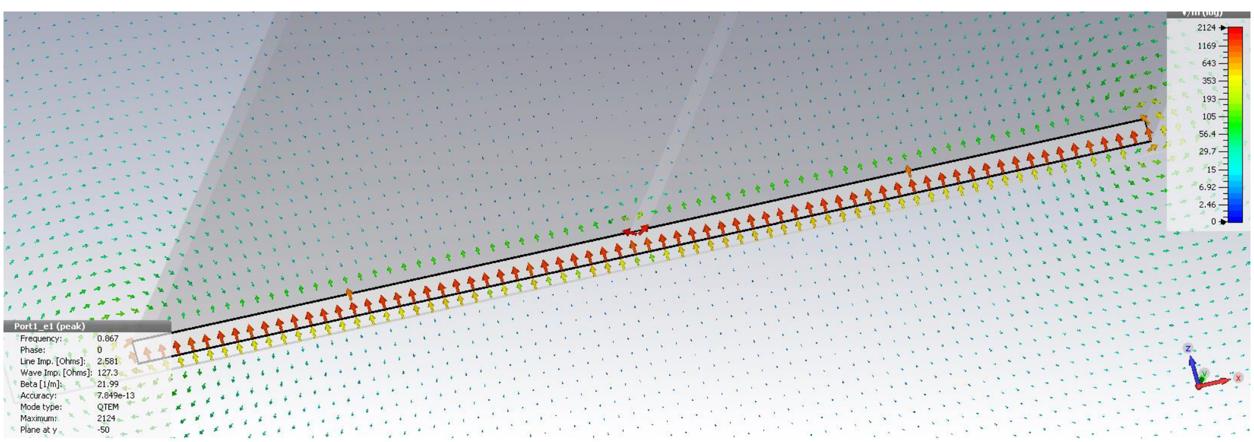

Figure 21. Simulation of the E-field of the common mode

As it can be seen, the E-field is propagated inside the structure and goes outside. It is clear that the highest electric field is at the inner of the structure. As you can see with the help of the arrows, the behavior of the electric field is the same as that expected for the dominant mode when the maximum intensity is in the middle similar a parabolic propagation.

The next mode, figure 22, has a similar behavior than TE_{20} mode, the same simulations have been made as in the previous case and the following results have been obtained.

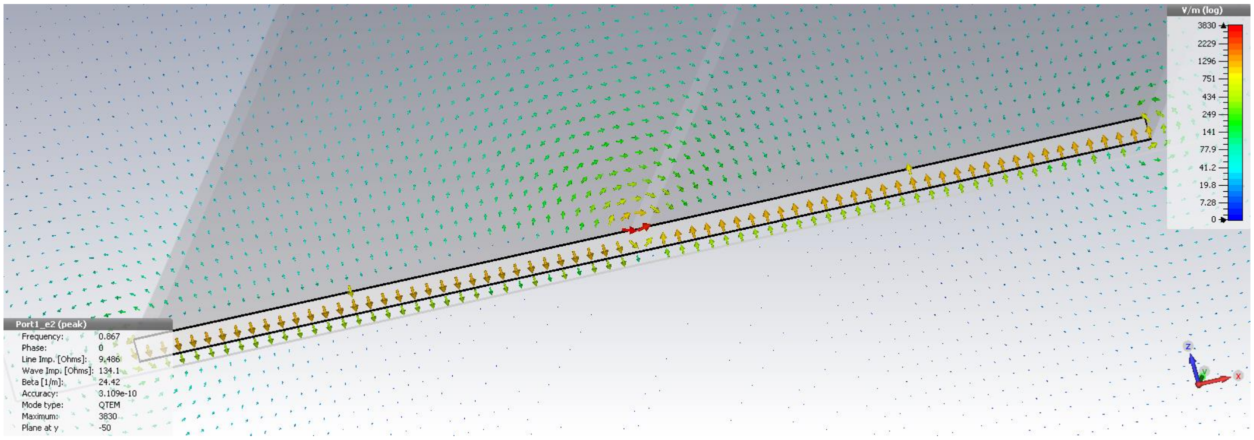

Figure 22. Simulation of the E-field of the differential mode

If you look at the scale, the intensity is higher than the last mode and the propagation field has a transversal behavior to the slot.

The β has a value equal to 21.99 $^1/_m$ and 24.42 $^1/_m$ and these values are very similar that the theoretical value calculated in the last chapter in equation (23).

Field intensity or field strength is a general term that usually means the magnitude of the electric field vector, commonly expressed in volts per meter. The graph of figure 23 shows the magnitude value (V/m) as a function of the distance (mm) which determines the maximum length were the field will be present from the confinement structure in the z-direction in both modes:

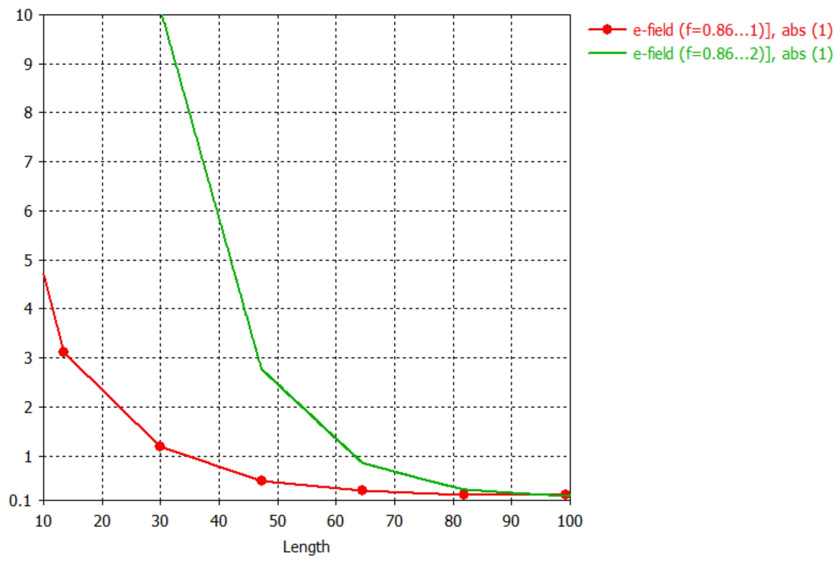

Figure 23. Magnitude graph

This field strength is obtained simulating an input power of 1W, which is the power at RFID reader works. The graph shows that it said before, the differential mode, represented with a green line, has more magnitude than the dominant mode, represented with a red line, because for example at 5 cm distance from the confinement structure, for a differential mode has a 2.5 V/m magnitude versus the 0.5 V/m magnitude in a common mode.

As shown in the graph, the electric field is obtained at least at 9 cm outside the structure, similar to the value that was expected and that was used to set the value of β in equation (24).

The RFID tag only need detect a minimum of 1 V/m in order to be activated. Therefore, for the common mode waveguide, it will have a maximum detection distance of 3.5 cm, while for the differential mode we will have a detection distance of 6.5 cm, almost twice as much as the previous mode.

More simulations have been designed for each mode, for this purpose, longitudinal and transversal cuts have been made in such a way that you can see more clearly how the electric field propagates through the structure. The images 24,25,26,27 shows the results in a 2D cut-plane.

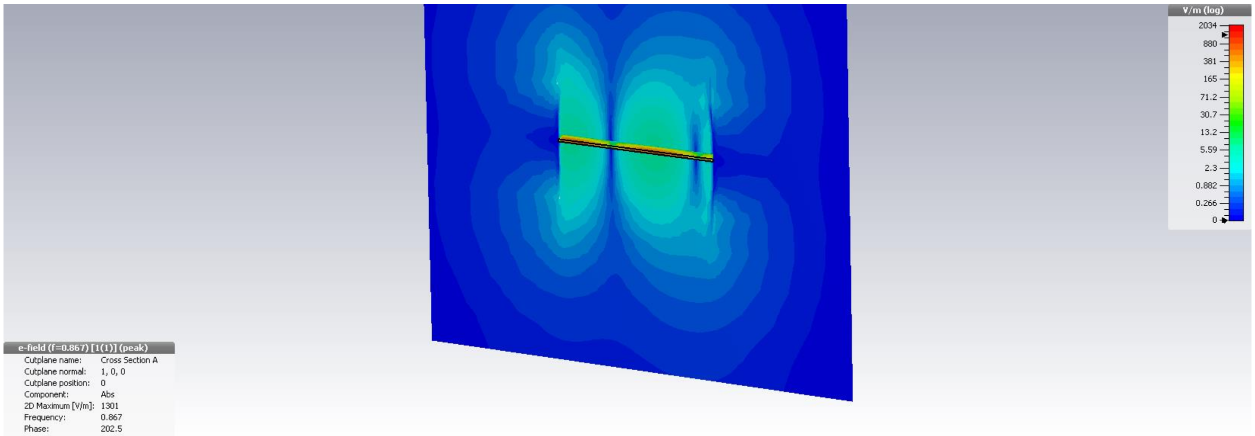

Figure 24. Cross section X common mode

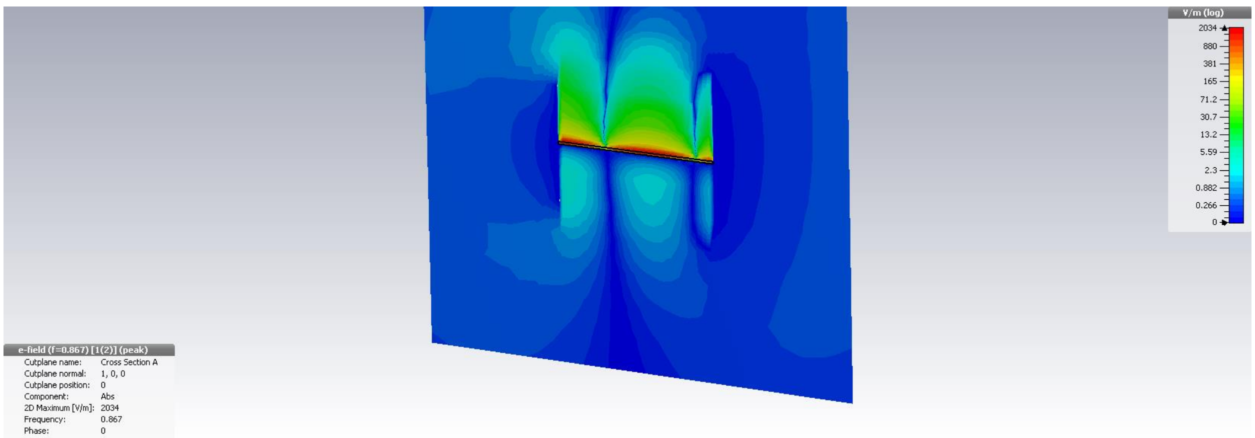

Figure 25. Cross section X differential mode

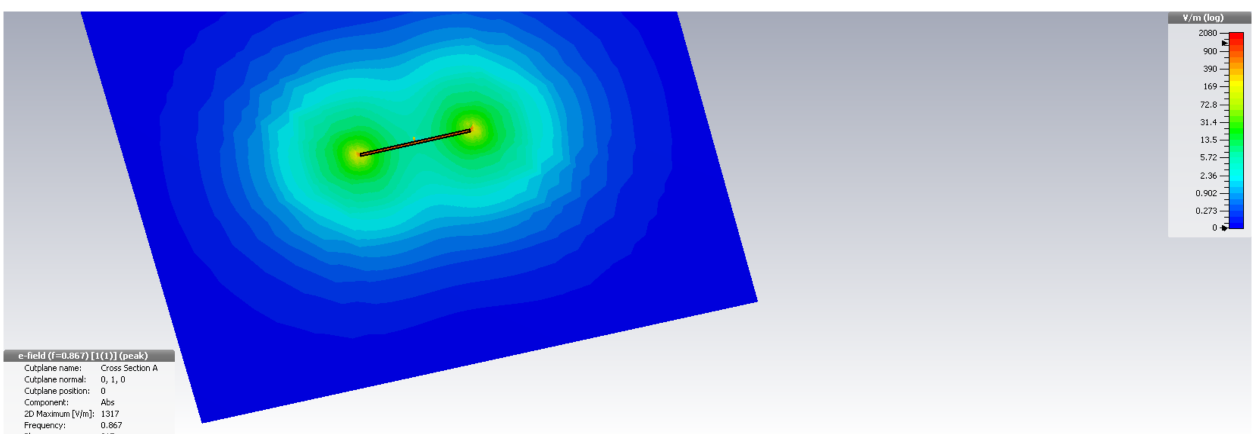

Figure 26. Cross section Y common mode

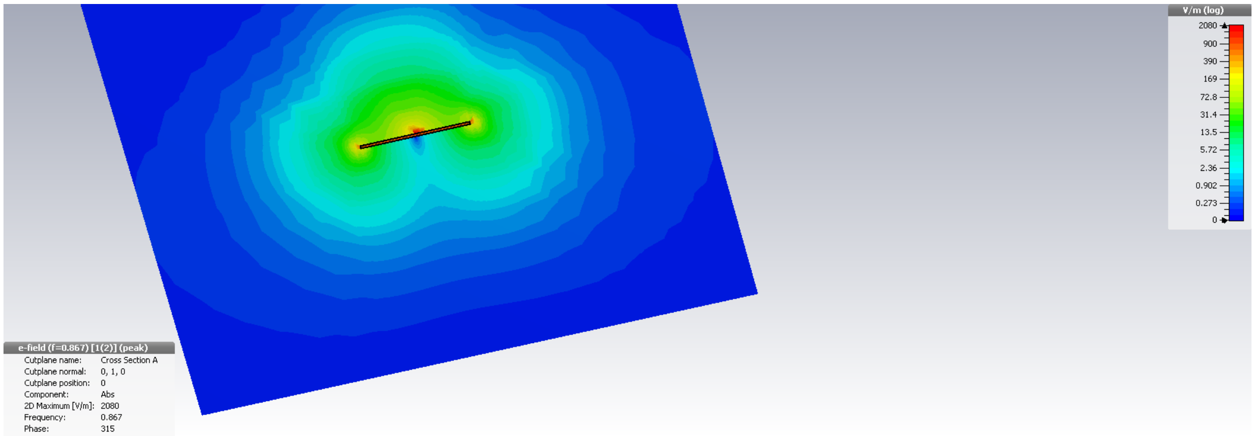

Figure 27. Cross section Y differential mode

The figures 24 and 25 show the simulation results at the longitudinal cuts, and it can clearly see how the wave propagates along the structure and how the E-field is radiated surrounding the structure.

As it said before and thanks that the scale has been adjusted equal for both modes, the differential mode has more intensity than common mode.

On the other hand, the figures 26 and 27 shows the simulation results at transversals cuts, and it gives us an idea of how the electric field radiates out of the structure.

In order to feed the structure is necessary design a transition between the rectangular waveguide and the power feed. For this reason is necessary create a transition lines to excite the structure. In addition, depends on how waveguide is fed, the ports will have a characteristic configuration.

The following point analyzes the port configuration to adapt impedance and the transitions needed to obtain the both modes, but without changing the width of the structure. For this part, first, the ports were designed in the CST software to see the different response that would be obtained.

3.4 Transition network design in CST

The CST Studio provide discrete ports, these ports consist of a single lumped element in the middle and two perfectly electric conducting wires connecting the port to the structure, and the S-parameters are calculated. The S-Parameter ports are the most frequently used port types and contain internal resistors for calculating S-Parameters with fixed reference impedances. These ports realize an input power of 1 W and enables the calculation of correspondent S-parameter

The procedure for creation these ports is to pick its two ends from the structure using the common pick tools and then to enter the characteristics to discrete port dialog box. It is simplified in the figure 28:

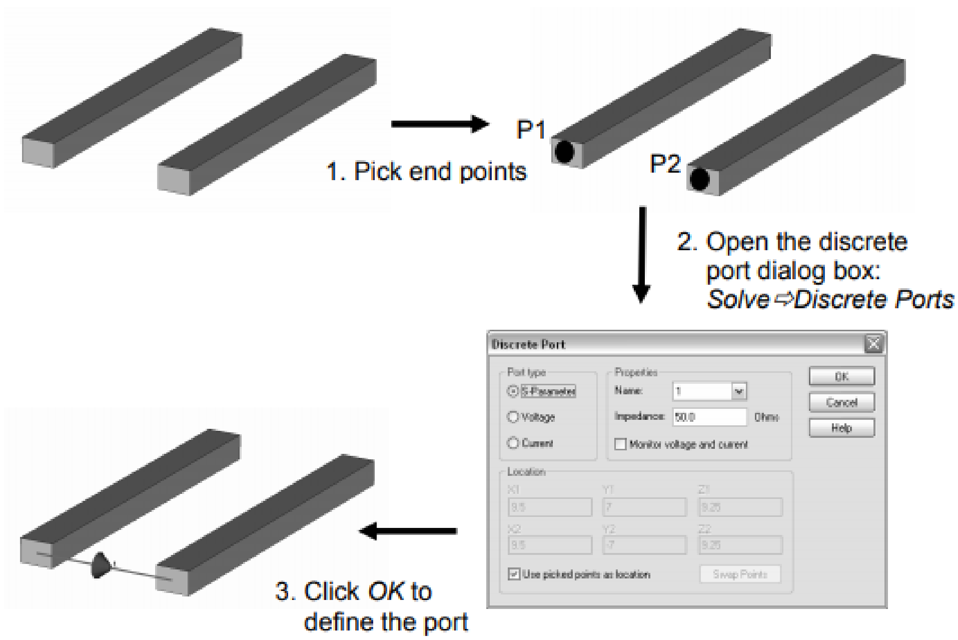

Figure 28. Procedure for creation discrete ports CST

3.4.1 Common Mode Simulation in CST

To simulate the common mode, its necessary to create the waveguide structure fed with the same phase. The CST does not have the option to create some ports in common mode, for this reason a transverse magnetic wall to the slot has been designed, dividing the geometry of the structure of confinement in two parts, so that it has simulated a half, because with the same geometry and properties the other half part will have the same behavior.

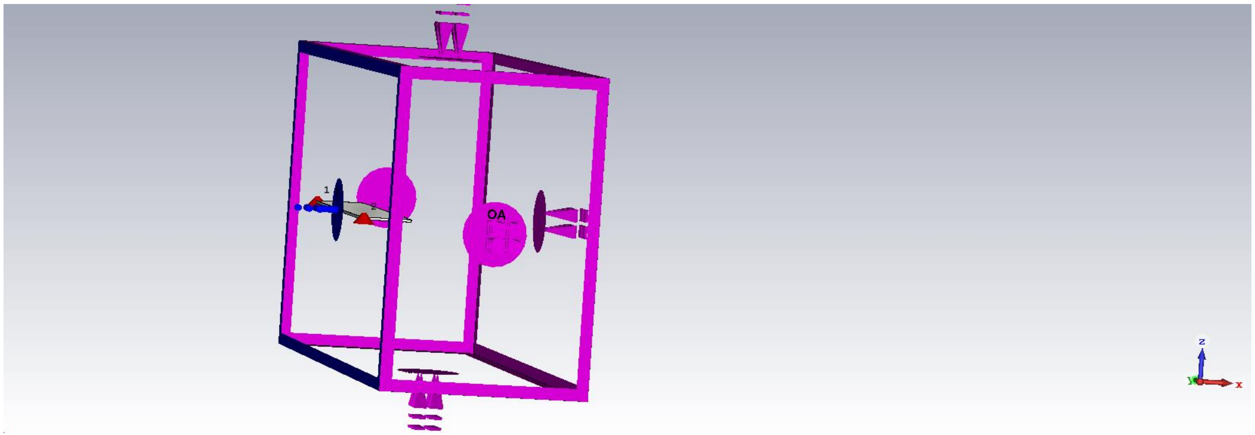

Figure 29. Magnetic wall common mode design

In this process, the characteristic impedance (Z_o) of the ports has been set to 50 Ω to give it greater functionality and that it is capable of being implemented in most systems. with this characteristic impedance.

Once the ports of the structure have been designed, the simulation done in CST obtain the next S-parameters. Tuning de ports along the width of the structure and fixing its characteristic impedance, it is obtained the next S-parameters in the figure 30.

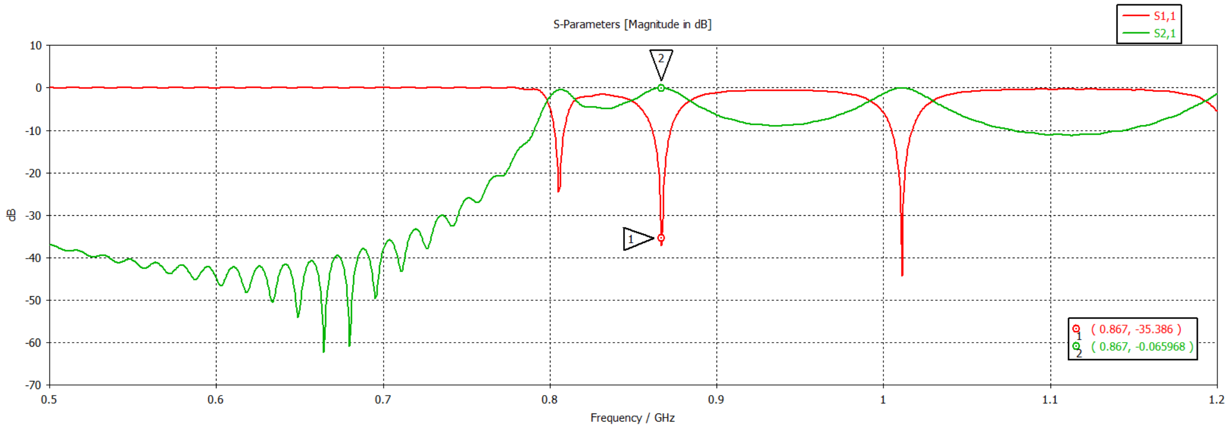

Figure 30. S-Parameters of common mode simulation in CST

It can be seen at the operating frequency we get a good reflection value S_{11} equal to -35.386 dB and a transmission coefficient equal to S_{21} equal to -0.066 dB.

3.4.2 Differential Mode Simulation in CST

To simulate the differential mode, its necessary create the waveguide feed structure with the discrete ports.

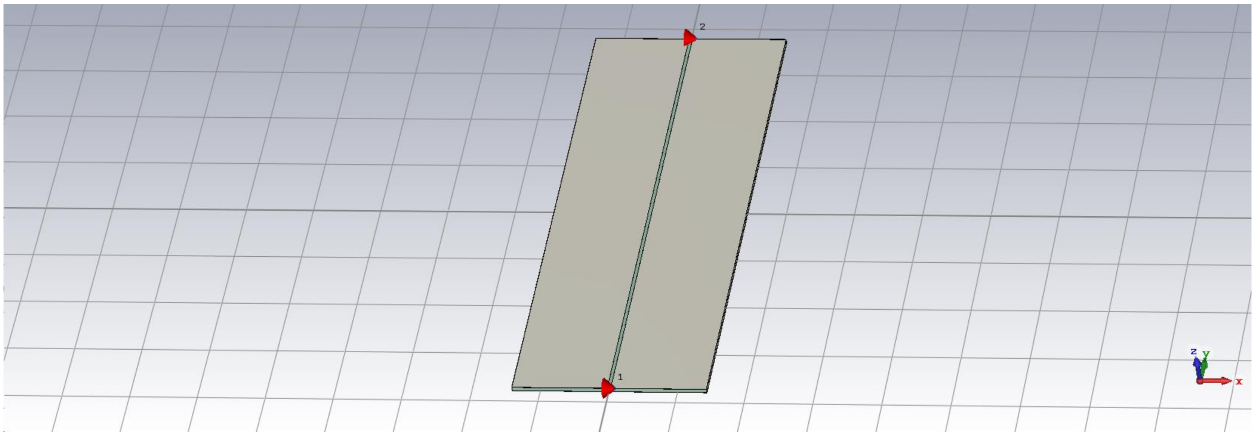

Figure 31. Differential mode design

Note that the orientation of the discrete port is used to determine the phase of the S-parameters. As depicted in figure 31, on one side you get a symmetry with a positive phase and on the other side you get a symmetry with a changed sign.

Tuning the ports connection at a good adaptation, it has been found to a distance between the middle of the slot and an end of the port equal to 10 mm. The results are shown below in the figure 32.

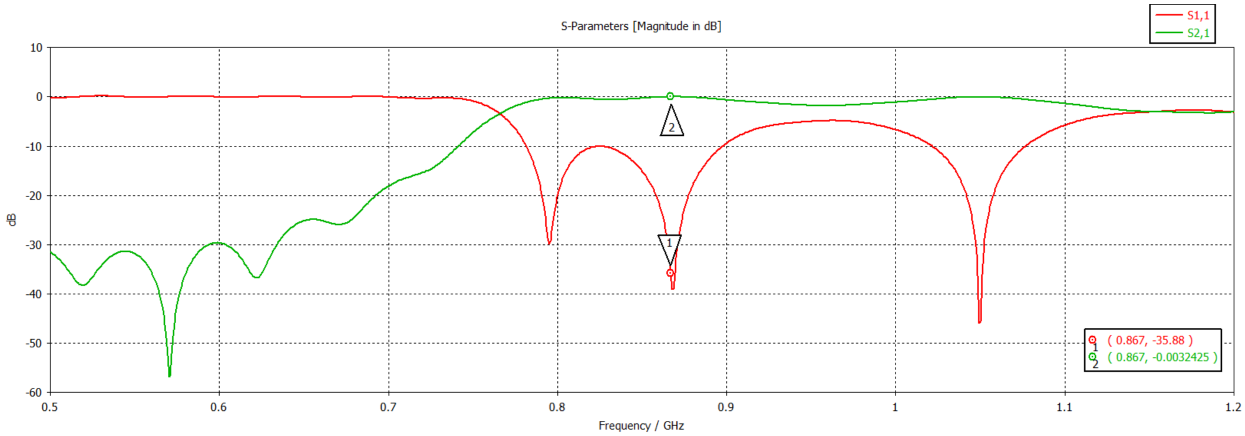

Figure 32. S-Parameters of differential mode simulation in CST

We can see the response of the circuits. At the operating frequency 867 MHz, it is obtained a very good return losses S_{11} = -35.88 dB, and the transmission coefficients S_{21} = -0.0032 dB.

It was also decided to design the adaptation between the ISM structure and the transition lines using ADS, as it is a more credible software for this type of flat structures.

Table 5 summarized the results obtained in the CST simulation.

S-Parameter (dB)	Common Mode	Differential Mode
S_{11}	-35.386	-35.388
S_{21}	-0.0032	-0.0032

Table 5. Summary S-parameters in CST

3.5 Transition network design in ADS

Substrate integrated waveguide technology has made it feasible to design low loss and low interference planar microwave structures. Transitions between SIW and other planar topologies like microstrip and coplanar waveguide are needed in order to excite and measure these structures. It is vital to provide low reflection transitions so that the component designs are independent of the influences of the transitions.

Whenever you want to excite or detect any mode, the method used should maximize the transfer of power between the source and the guide, or between the guide and the receiver.

These transitions are made up of transmissions lines and these might have different formats like microstrip or stripline. Then, we will explain these two formats of transmission lines, advantages and disadvantages for each format.

Microstrip routing is a transmission line trace routed on an external layer of the board. Because of this, it is separate from a single ground plan by a dielectric material. Stripline is a transmission line trace surrounded by dielectric material suspended between two ground planes on internal layers [15].

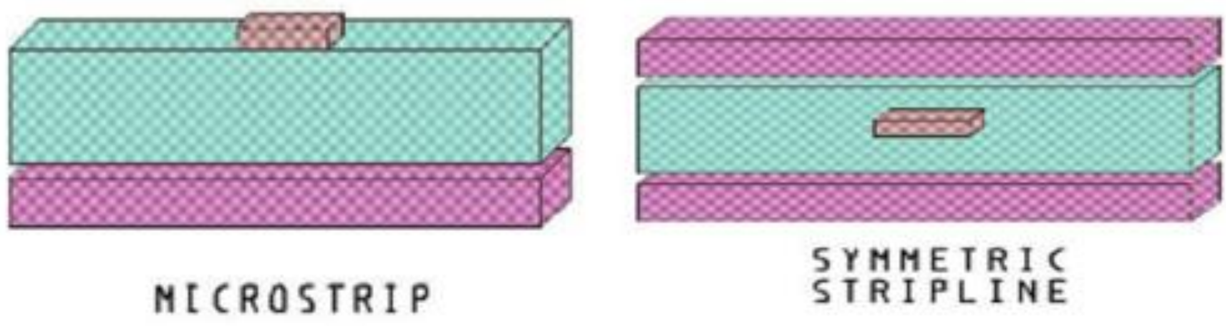

Figure 33. Microstrip and Stripline design

Now that the physical differences between stripline and microstrip transmission lines are known, the table 5 summarize the differences in order to choose which one should you use in the design.

Features	Microstrip	Stripline
Structure	Conducting layer, dielectric layer and ground layer	Top and bottom ground plane, dielectric layer, embedded conducting layer within dielectric
Characteristic Impedance	20 to 120 Ohm	35 to 250 Ohm
Width of line at same impedance	Wider	Narrower
Manufacturing tolerances	Tighter	Lighter
Radiation Loss	High for low ε and Low for high ε	Low
Dielectric Loss	Less	More
Dispersion	Low	None
Component mounting	Easy for series and difficult for shunt	Very difficult because of totally covered structure
Advantages	• Smaller size • Easy to fabricate • Easy to troubleshoot	• Good EM shielding can be achieved with this structure • Low attenuation loss

		• Wider bandwidth • Better isolation
Disadvantages	• Unwanted radiation in uncovered microstrip based configuration • Higher loss • Poor isolation among adjacent lines	• Complex and expensive in fabricating it. • Stripline Trace width is smaller compare to microstrip line of same impedance and height. • Tuning or troubleshooting is complex.
Applications	It is preferred to use in miniature microstrip patch antennas due to their radiating structures.	It is preferred to use in multilayer circuits via PTHs (Plated Through Holes) since it is easy to route signals between layers.

Table 6. Microstrip vs Stripline

Based on table 5 and the critical characteristics like price, easy to fabricate, how it has said before, the microstrip will be the format of the transmission line.

The microstrip line is very practical in many configurations, including active components connectivity, the trend is to merge it in the same substrate with SIW, geometrically irreconcilable structures. This requires the development of transitions, junctions and couplings. These transitions are very important for the matching of impedance and field between the SIW and planar circuits [16].

Depends on the mode that the waveguide is working, the transition network created will be different. It has been decided to simulate the transition design using ADS software. Remember that for each design the substrate is Rogers 3010, so before starting with the design of each transition it is advisable to show the configuration of the substrate used.

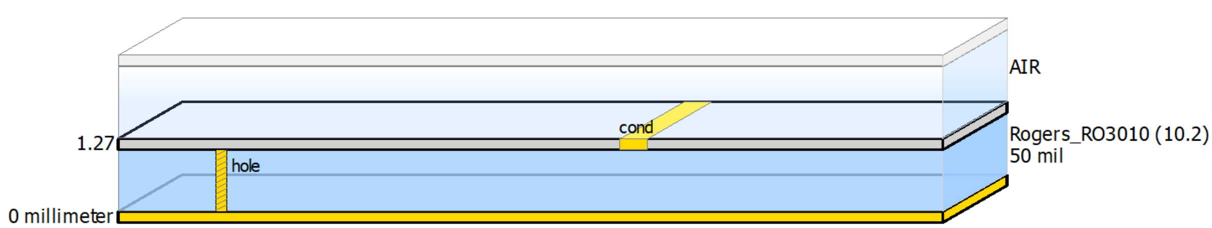

Figure 34. Layout Components ADS

	Type	Name	Material	Thickness
	Dielectric		AIR	
1	Conductor Layer	cond (1)	Copper	35 um
	Dielectric		Rogers_RO3010	50 mil
	Cover		PERFECT_CON...	0 um

Table 7. Layout Components

In many cases, loads and termination for transmission lines in practical will not have impedance equal to the characteristic impedance of the transmission line. This result in high reflections of wave transverse in the transmission line. For this is designed an impedance matching to deliver maximum power from the source to the load.

3.5.1 Common Mode Simulation in ADS

To achieve good impedance matching and small return loss the proper transition between microstrip line and SIW is important. A tapered transition is appropriate and is useful in most applications [17] [18]. Despite that, the design process of this transition requires multiple full-wave simulations, because optimization is the strategy of choice to solve this problem.

In order to transfer the power, the microstrip taper line is connected to the feed waveguide.

The figure 35 represents a microstrip taper transition from microstrip line to SIW structure.

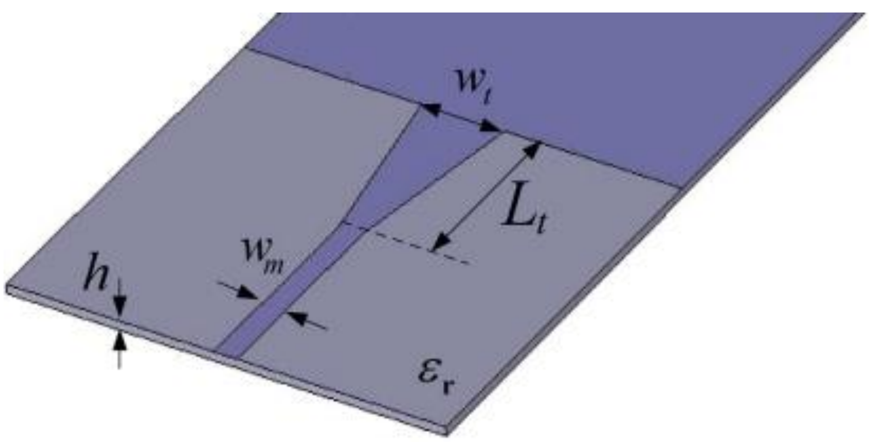

Figure 35. Taper Transition concept

Where w_m is the width of the microstrip line, w_t is the tape width, L_t is the taper length and h is the substrate height.

First it is necessary choose the width of the microstrip w_m line in order to excite and integrate the SIW structure with a microstrip port, so the characteristic impedance of the microstrip line becomes 50 Ω like in CST design.

First, it has been designed the layout with the Momentum for this transition with the structure, as it shown in figure 36.

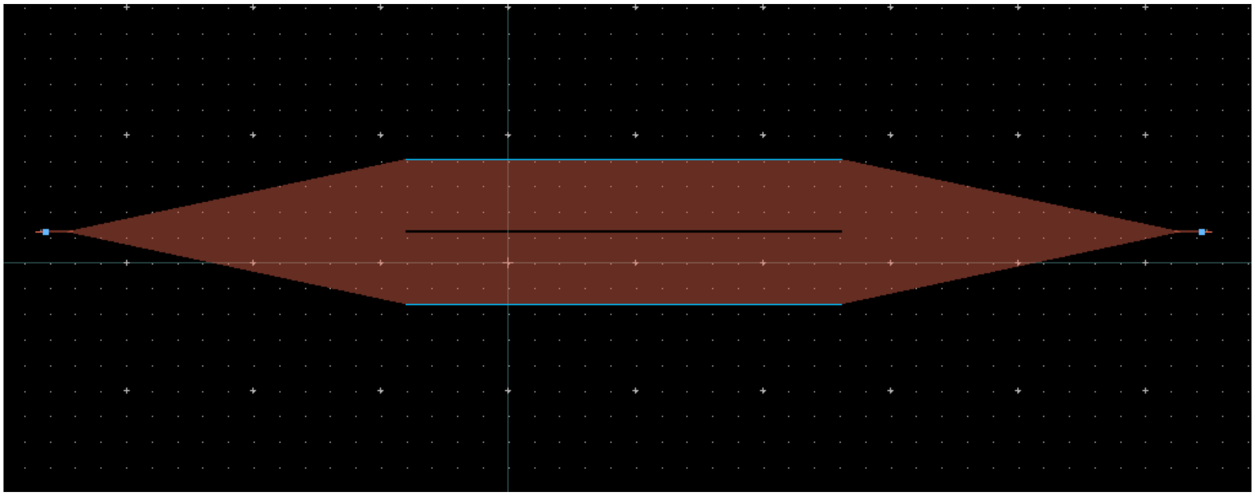

Figure 36. Layout Common mode ADS

The central slot of the structure is easily recognized, and if you look at the design on the sides of the structure you can see two blue lines. These lines are made of conductor and represent the sidewalls of the waveguide, necessary for SIW technology in order to connect the conductor on top and bottom. It has been designed, at the ends of the tappers, two ports with a $Z_o = 50\Omega$.

It is notable that the length of the taper line, 133.5 mm, controls the return loss of the structure. The total length of the structure is equal to 453.5 mm. It is mentioned that the taper length is integer multiple of guided quarter wavelength. For this reason, several simulations have been made, such as sweeping the width of the taper and the length, and in this way the tapper dimensions has been fixed in the best adaptive case. Next, is shown the S-parameters results in figure 37.

Note that with the simulation done directly in Momentum, the losses of the substrate and conductor are taken into account, in addition to other factors that degrade the value of the S parameters of adaptation.

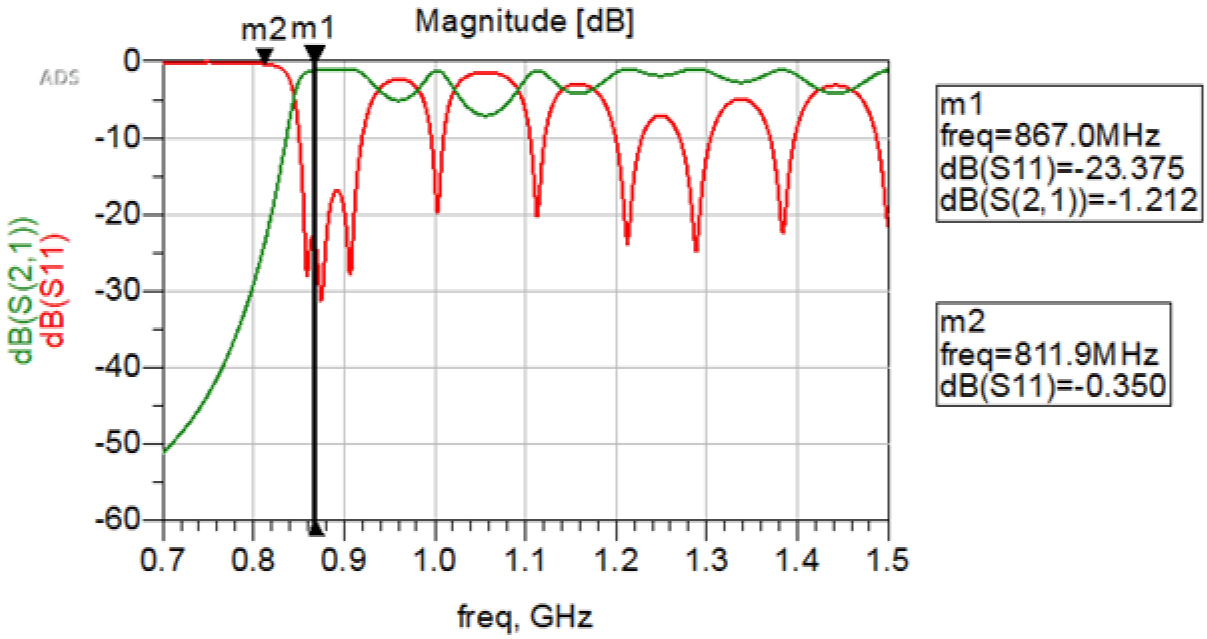

Figure 37. S-Parameters Common mode ADS

As depicted, at the operating frequency 867 MHz, how the marker 1 indicates, the S_{11} and S_{21} has -23.37 dB and -1.21 dB respectively. The results show a good matching at the operation frequency to reference impedance. Something else that is important is that the cut-off frequency 811.9 MHz is very close to the calculated in the equation (28).

3.5.2 Differential Mode Simulation in ADS

To feed the structure in differential mode, a divisor has been designed as it shown in figure 38. This divider allows having a balanced outputs and adapted ports inputs.

It has been designed a transformer used to connect two single-ended with equal potential with 180 degrees phase difference, to unbalanced transmission line, like a balun transition.

It is important to know the concept of matching, which is mean to the relationship between a wave transmitted by a port and the wave reflected that we receive by this same port, to have the rest of ports loaded with an impedance reflected. For our divisor, we want that the matching in the ports is zero we do not have reflection of the wave transmitted by the ports.

In case of referring to the transfer of power between the input port and the output ports, we are quantifying the relationship between the power transmitted by the port of entry 3, and the power we have in the ports of exit 1 and 2. In our divider, this value will be important because it is the efficiency of our divisor. In case of having a 3-port splitter, the objective is to be able to have a transfer of -3dB, corresponding to half the power.

Therefore, the characteristic impedance of the port 3 is 50Ω, that is way the port 1 and port 2 must be have an impedance equal to 25Ω and the same magnitude but with different sign for the other port.

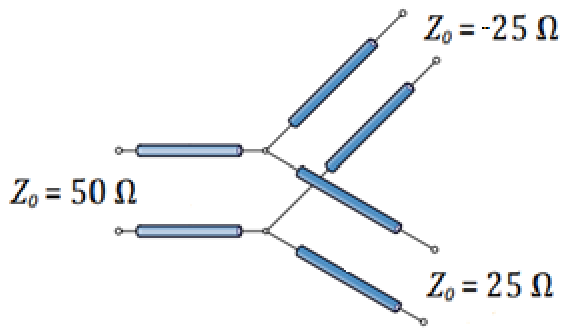

Figure 38. Impedance Matching Divider

In order to known the dimension of the transmission lines, it has used the LineCalc Tool. The figure 39 shows how it has designed the dimension of the transmission line.

For this degenerate mode, how it has been explained in the past section, the transition must be powered the waveguide with a mismatch off 180º between port 1 and port 2. Consequently, one line will have an electrical length of 90º and the other line will have an electrical length of 270º.

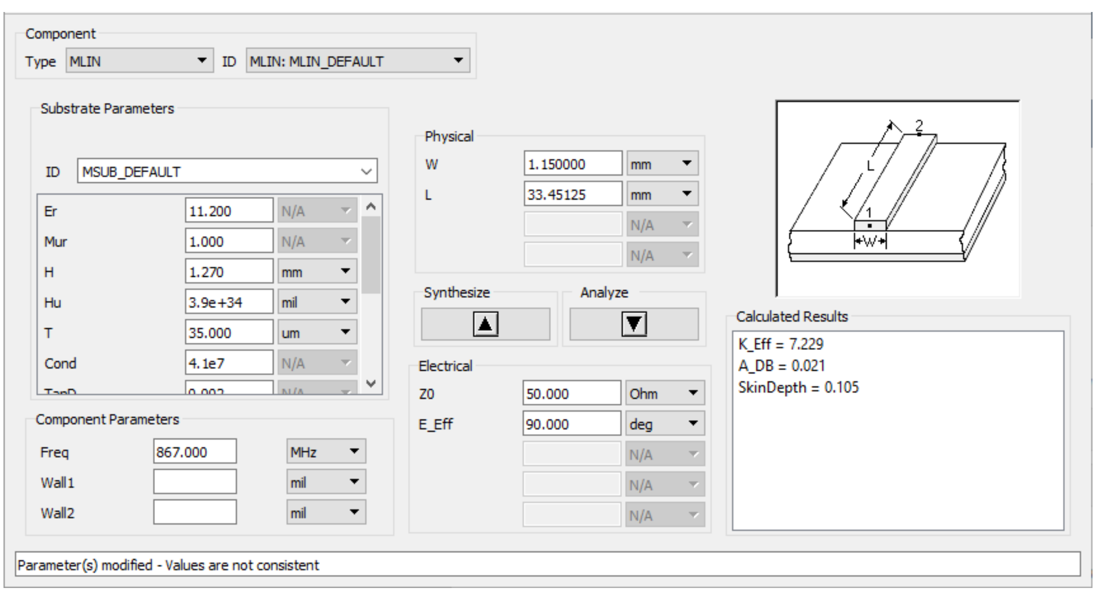

Figure 39. LineCalc Transmission Line 90°

As it can be seen, once the substrate parameters, electric length and characteristic impedance have been added, it has been obtained a width equal to 1.15 mm.

The length of the line for each case is:

$$90° \rightarrow 33.45 \text{ mm}$$

$$270° \rightarrow 100.34 \text{ mm}$$

Once the dimensions and the characteristics impedance have been obtained, the next step is to create the layout. As one line is longer than the other, to miniaturize the design, the longer line has been designed in the form of meander line, and how we are working in low frequency, we would have no coupling effects between the lines.

First, it was designed the schematic circuit in order to see the functioning of the divider in ideal mode and visualize circuit results. For this, the following basic schematic is assembled in the figure 40.

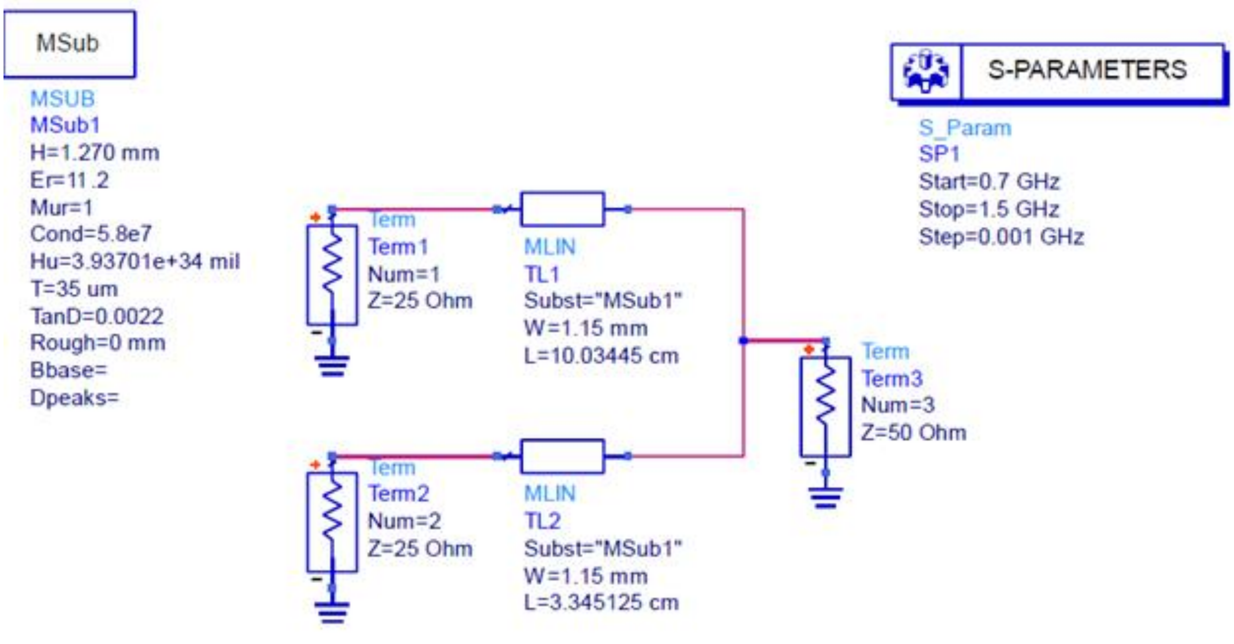

Figure 40. Differential mode Schematic

Once the frequency values of the simulation, the characteristics of the dielectric, the value of the impedance of each port and the dimensions of the two transmission lines were fixed, the following ideal results, represented in figure 41 and 42, have been obtained.

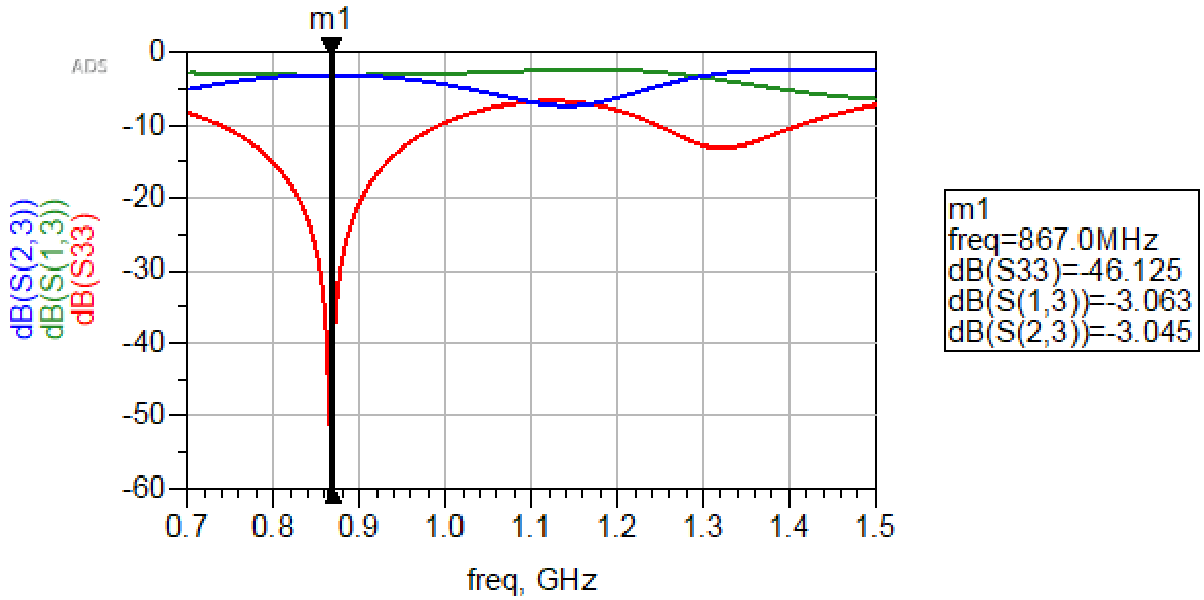

Figure 41. S-Parameter ideal differential mode transition

At the operating frequency, a good matching has been achieved a good adaptation in port 3 with values of S33 equal to -46.125 dB and S13, S23 close to -3 dB which was expected, corresponding to half the power.

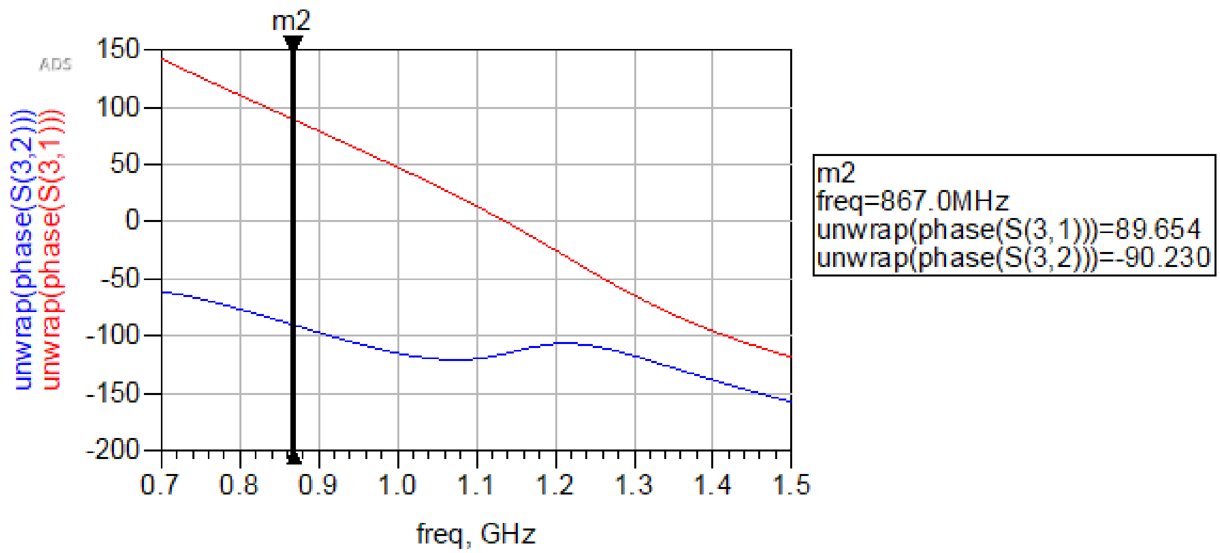

Figure 42. Phase of transmission lines

Regarding the phase between the two transmission lines can be seen in figure 40, we get on the one hand a phase equal to 89.654 while on the line of the meander we get a phase of -90.230, thus getting a phase shift between both lines close to 180º desired.

The next figure 43 shows the layout designed:

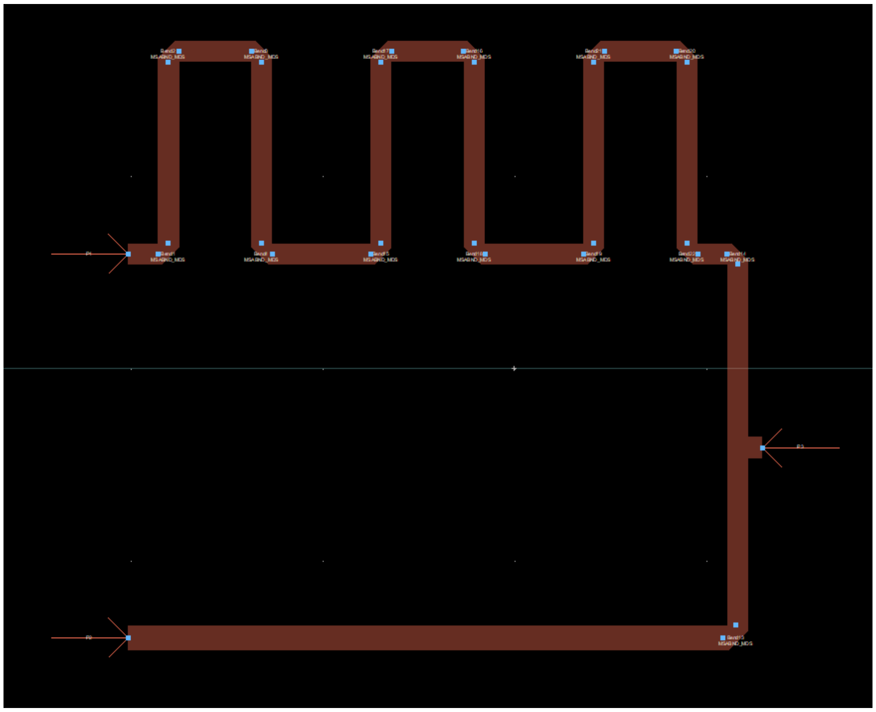

Figure 43. Layout Differential mode transition ADS

Note that, the distance between the two transmission lines is equal to 20 mm and is the same value that it has been found in CST. By tuning the dimensions of the lines a little, the transition has been adapted and the following results, represented in figure 44 and 45, have been obtained.

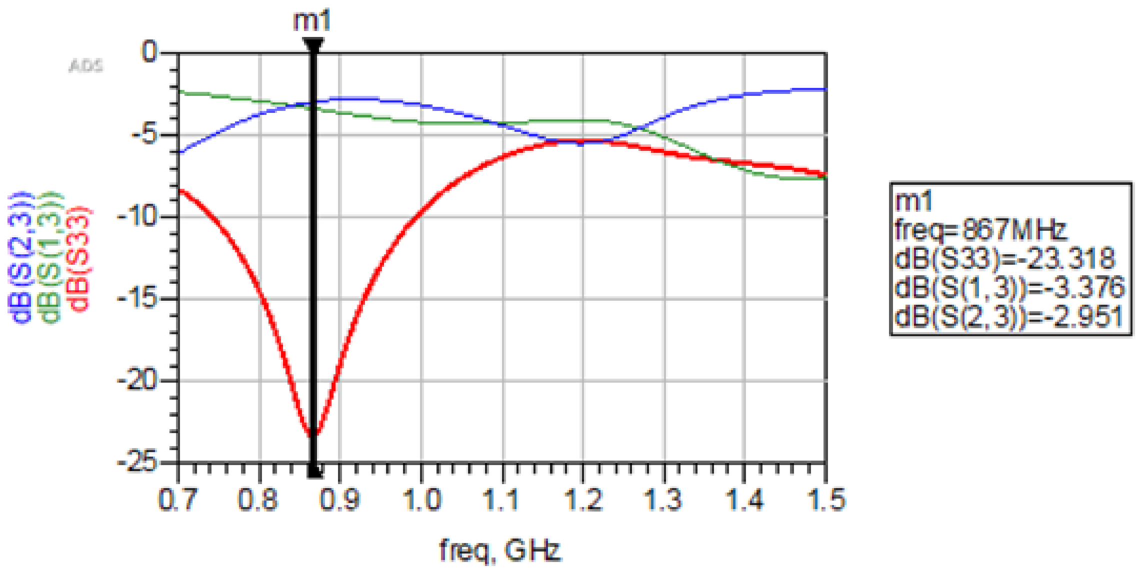

Figure 44. S-Parameters Differential Mode Transition

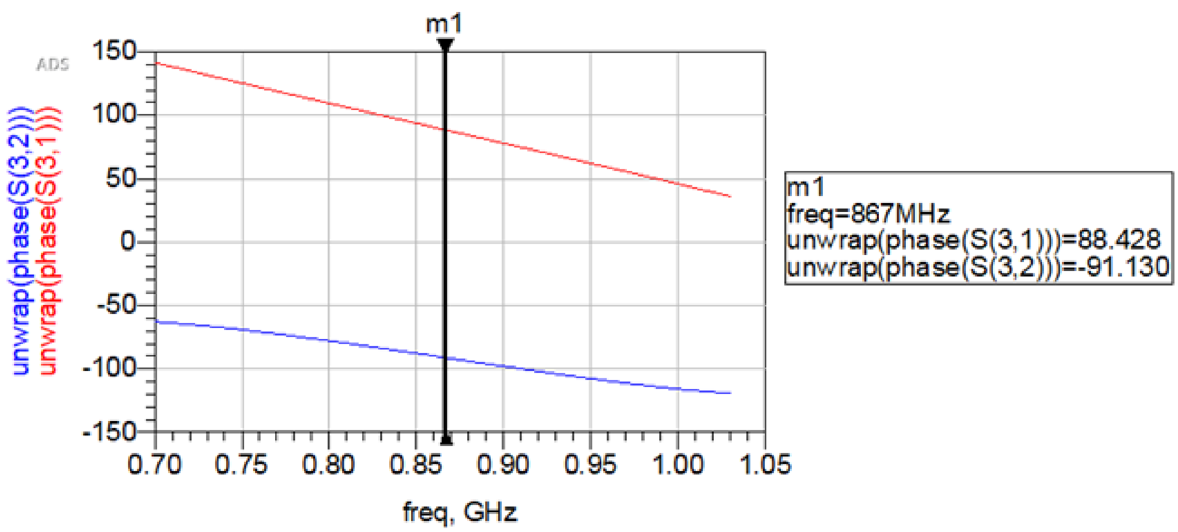

Figure 45. Phase Differential Mode Transition

As can be seen, the results show a good response below 20 dB for our operating frequency. The table 7 shows a summary of the ideal and simulated data at Momentum.

	S33 (dB)	S13 (dB)	Phase S23	Mismatch
Ideal simulation	-46.125	-3.063	-3.045	179.884
Momentum simulation	-23.318	-3.376	-2.951	179.558

Table 8. Ideal results vs Momentum results

Once the transition is designed and analyzed, the simulation of the complete set between transition and structure will be implemented in figure 46, and the values obtained from the simulations performed will be analyzed in figure 47.

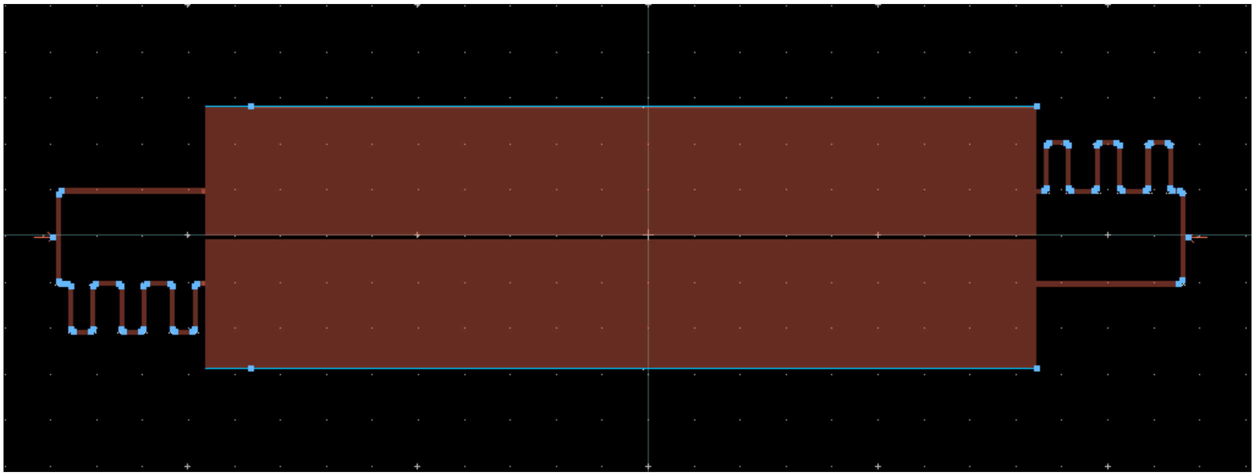

Figure 46. Layout Differential mode ADS

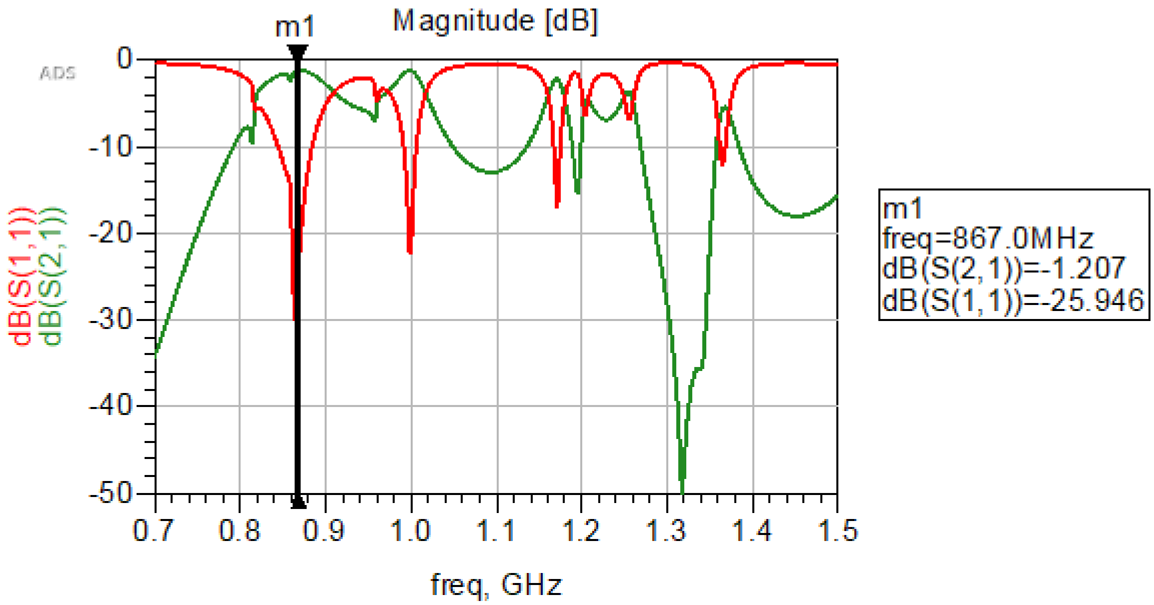

Figure 47. S-Parameters Differential mode

As it can be seen in figure 47, a good impedance matching to reference impedance is appreciated since the S_{11} parameter is below -25 dB at the operating frequency. The measured S_{21} parameter shows an insertion loss of -1.2 dB at 867 MHz. Once all the simulations have been obtained, the fabrication of the device will be carried out in order to be able to measure it and compare the practical results with the theoretical ones.

4. Fabrication Process and Simulation

This chapter pretends to validate the previous simulated results. To do so, the last two prototypes studied in the previous section will be implemented, the model with the tapper simulating el dominant mode and the mismatched model simulating the degenerate mode. Once the layout is finished in ADS, the file is imported as DXF field to be printed.

Both circuits were milled with the LPKF Protomat H100. is an advanced PCB prototyping plotter that includes many new features derived from high volume production systems. The ProtoMat H100 provides the maximum capability for completing complex prototyping jobs on time and within budget. The speed and resolution enhancements come from the combination of a 100,000-rpm milling motor along with a precise board positioning system and X-Y motion controller. Resolution is also increased by a camera vision system that accurately positions the milling head by locating board alignment fiducials. A result of this superior resolution is high artwork definition, which improves multilayer milling.

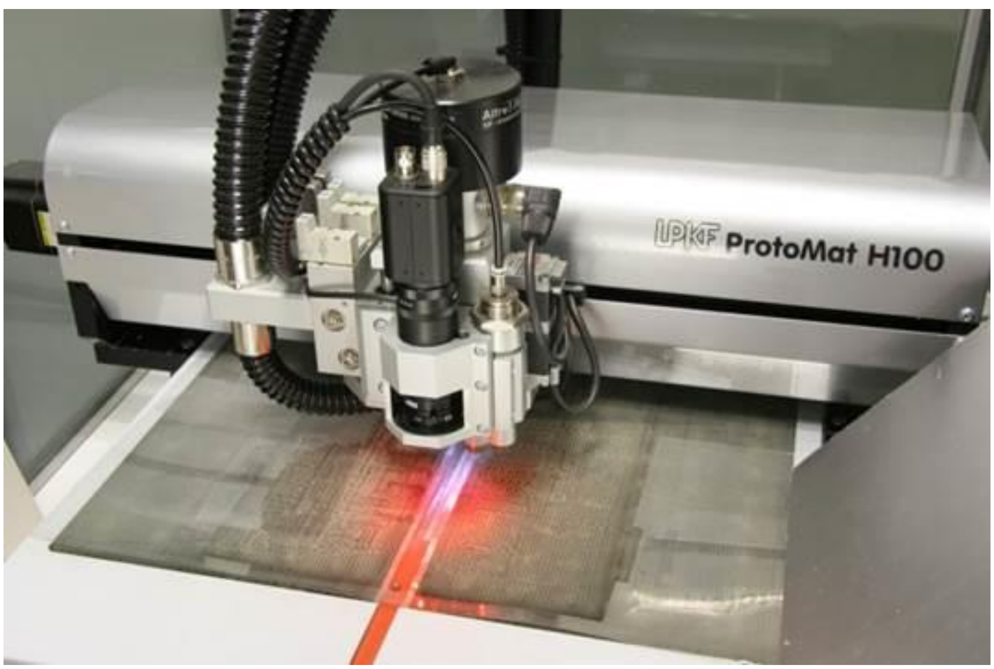

Figure 48. LPKF ProtoMat H100

Once the PCB has been milled, SMA female impedance connectors are soldered to the ports 50Ω. These ports will allow us to connect the printed circuit to the network analyzer to obtain the S-parameters.

Figure 49. Network Analyzer

It is a four-port analyzer with which we can obtain from a single measurement the complete matrix of 16 values. Otherwise we should load ports to 50 and measure the prototypes.

4.1 Common Mode Prototype

For this common mode prototype, for laboratory reasons, it is not possible to manufacture a prototype whose length is more than 300mm. Remember that the length is 453.5 mm. Therefore, it has been decided to reduce all dimensions values, including the dielectric thickness inches, by half in order to be able to manufacture it. With this technique, it is possible to carry out the different simulations, but the frequency of operation will be located at twice the previous one. So, if before the operating frequency was 867 MHz, now the new operating frequency is located at 1.734 GHz.

The negative point is that for this prototype it will not be possible to check if it can excite a RFID tag because we are at another frequency.

Therefore, you must first simulate with the new operating frequency, the figure 50 shows this.

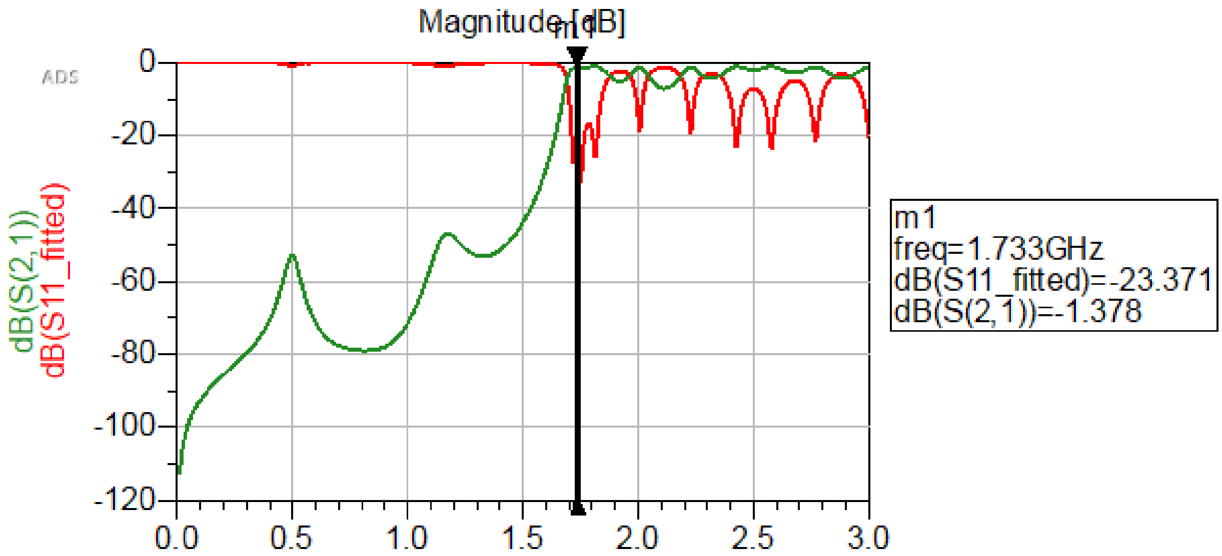

Figure 50. S-Parameters Common Mode rescaled

The S-Parameters, S_{11} values equal to -23.371 dB and S_{21} is equal to -1.378 dB, are obtained. If these results are compared with those obtained in figure 37, we can see the same behaviour and almost the same S-parameters, but at a double operating frequency.

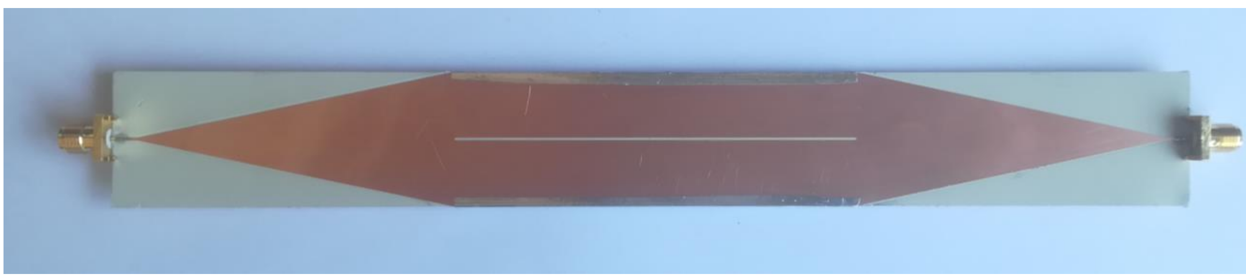

Figure 51. Common Mode Prototype

As it can be seen in figure 51, in the sidewalls of the waveguide structure there is a metallization necessary for SIW technology in order to connect the conductor on top and bottom.

Respect S-parameters measured, in the figure 52 you can see the measured results and the results of the simulation, and table 9 summarizes all the measurements obtained.

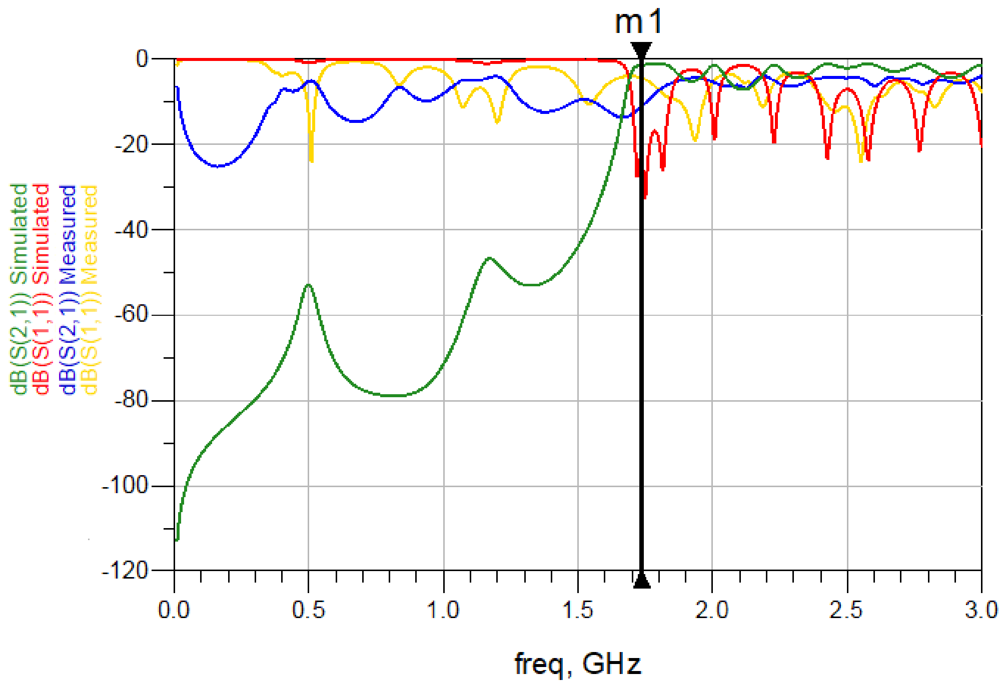

Figure 52. S-Parameters Common Mode results

S-Parameter (dB)	Simulated	Measured
S_{11}	-23.371	-4.338
S_{21}	-1.378	-11.045

Table 9. Comparison between simulation and measurements, Common Mode

According to the results obtained, we do not obtain the same real measures as the simulated ones.

4.2 Differential Mode Prototype

For this prototype, figure 53, it has been designed exactly with the DXF file exported from ADS.

Figure 53. Differential Mode Prototype

The S-parameters measurements of this prototype displays, as it can be seen in figure 54, a great difference with the expected behavior in the software simulation.

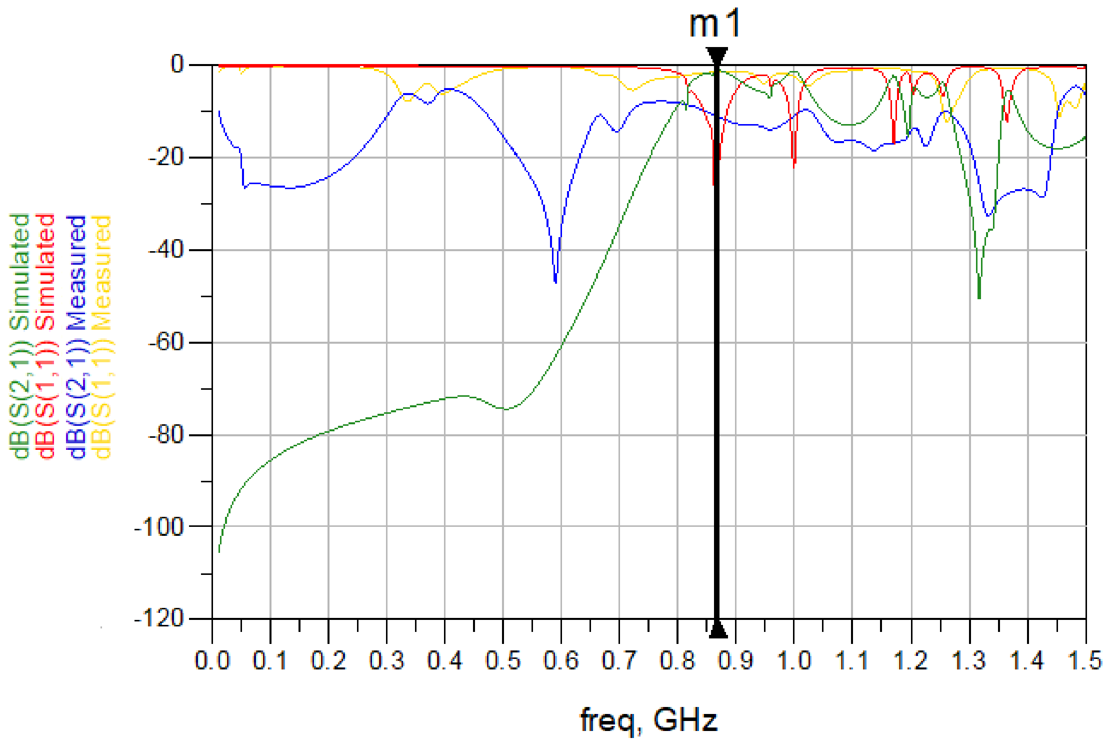

Figure 54. S-Parameters Differential Mode results

The table 10 shows the results of the measures obtained versus the results simulated by software, both at the same operating frequency.

S-Parameter (dB)	Simulated	Measured
S_{11}	-25.946	-1.412
S_{21}	-1.207	-11.113

Table 10. Comparison between simulation and measurements, Differential Mode.

As evidence, the results in both prototypes are completely different with the simulations. It has been ensured that the ports function correctly, the soldering of the SMA connectors has been looked microscope and no faults have been identified.

As can be seen in figure 52 and figure 54, in the measured results, we see that at low frequencies, there is a transmission. For this reason, it is believed that the sidewall that acts as vias for the top and bottom, is not doing its function correctly and it has been tested to create this short circuit with conductive ink as seen in the image 55.

Figure 55. Prototype with conductive ink

Unfortunately, no other method has been able to achieve a correct matching or similar with the simulated.

In the moment where this report was submitted some options to solve the discrepancy between simulation and measurement, based on the improvement of the conductivity of the sidewalls of the waveguide, are under consideration.

5. Conclusions and Further work

5.1 Conclusions

The main objective has been achieved by the simulation of the waveguide for electromagnetic confinement. This waveguide has been designed using SIW technology for an operating frequency of 867 MHz.

The study revealed that according to the power design of the waveguide, different propagation modes are produced, achieving an improvement in the coverage area for the detection of RFID tags. Therefore, two prototypes have been designed. For the first prototype, called common mode prototype, a taper transition has been designed and for the second prototype, a balun transition has been designed.

Theoretically found the dimensions were simulated with the assistance of powerful electromagnetic simulation software CST Studio which allows to analyze the field distribution. Good results have found for both waveguide prototypes, achieving a maximum detection distance of 3.5 cm for common mode prototype, while for the differential mode prototype will has a detection distance of 6.5 cm.

To simulate the design of the transitions from SIW to microstrip in terms of matching, ADS software has been used. Good results similar to those expected have been obtained for both prototypes.

Once all the simulations were done, both prototypes were made. The results obtained are not as expected. Due to this, we have not been able to do a functional test because the antenna receives a lot of reflection and the prototype cannot connect.

So finally, we can conclude that the waveguide has the expected results in the simulations but no good results have been achieved in the real measurements.

5.2 Further Work

The further work of this project consists in 3 different options

Achieve real measurements according to the simulated results in the different simulation software.

Due to the limited time to deliver the work, it has not been possible to make a single structure that can work on both modes of propagation proposed in this work. For this a possible solution, would be to design the same circuit, and between the two transitions for each mode put a SPDT switch to choose the mode of propagation.

Other option there is a possibility a miniaturization the transition in order to increase the waveguide structure and for this way, cover more area and possibilities of detection of the RFID tag. One possibility would be to change the type of substrate, which leads to the electrical permittivity changing and this would affect the dimensions.

6. References

[1] X. Qing, C.K. Goh and Z.N. "Chen Segmented loop antenna for UHF near-field RFID applications"

[2] F. Paredes, G. Zamora, F. J. Herraiz-Martinez, F. Martín and J. Bonache, "Dualband UHF-RFID Tags Based on Meander Line Antennas Loaded with Spiral Resonators", *IEEE Antennas and Wireless Propagation Letters, vol. 10, pp. 768– 771*, July 2011

[3] Philips Semiconductors 'Item-level visibility in the pharmaceutical supply chain: a comparison of HF and UHF RFID technologies', July 2004

[4] D. G. Hall, "Vector-beam solutions of Maxwell's wave equation," *Optics Letters 21 (1), 9-11* 1996.

[5] Benenson-Harris-Stocker-Lutz, "Handbook of Physics", 2002:

[6] D. M. Pozar, "Microwave Engineering", 3ª Ed, Wiley, 2005.

[7] , A. Flores-Pérez, J. Hernández-Hernández, S. Hacyan, R. Jáuregui K. Volke-Sepulveda, "Transverse electric (TE) and transverse magnetic (TM) vector vortices in free-space: analysis and experimental generation*", Instituto de Física, UNAM,* June 2009

[8] J. Turunen and A.T. Friberg, "Electromagnetic theory of reflaxion fields," *Pure Appl. Opt. 2, 539-547*, 1993.

[9] Edison Coimbra Gutiérrez, "Antenas y propagación de ondas, Tema 3", 2010

[10] E.Jensen "Cavity Basics" *CERN, Geneva, Switzerland*, 2009

[11] M. Bozzi, L. Perregrini, K. Wu, and P. Arcioni, "Current and future research trends in substrate integrated waveguide technology," *Radioengineering, vol. 18, pp. 201-209*, June 2009.

[12] Haiyan Jin, Yuliang Zhou, Yong Mao Huang, and Ke Wu, "Slow-Wave Propagation Properties of Substrate Integrated Waveguide based on Anisotropic Artificial Material*" DOI 10.1109/TAP.2017.2726688 IEEE Transactions on Antennas and Propagation*, 2017

[13] K. Wu, D. Deslandes and Y. Cassivi, "The Substrate Integrated Circuits - A New Concept for High-Frequency Electronics and Optoelectronics," *TELSKIS 2003*, Nis, Serbia and Montenegro, pp. Oct. 2003.

[14] Jordi Bonache, Gerard Zamora, Ferran Paredes, Simone Zuffanelli, Pau Aguilà & Ferran Martín, "Controlling the Electromagnetic Field Confinement with Metamaterials" *DOI: 10.1038 Scientifics Reports*, November 2016.

[15] Ruzhdi sefa, Arianit maraj "Analysis and design of microstrip to balanced stripline transitions".

[16] D. Deslandes, K. Wu, "Integrated microstrip and rectangular waveguide in planar form," *IEEE Microwave and Wireless Components Letters, VOL. 11, NO. 02, 68–70,* 2001.

[17] Dominic Deslandes, "Design considerations for tapered micro strip to substrate integrated waveguide transitions," *IEEE Trans. Microwave Theory & Tech., vol. 46, no.5, pp.625-630,* May 1998.

[18] Muhammad Imran Nawaz, Zhao Huiling "Substrate integrate waveguide to Microstrip transition at X-Band".

7. Annex

ROGERS CORPORATION

Data Sheet

Property	Typical Value[1]				Direction	Unit	Condition	Test Method
	RO3003	RO3035	RO3006	RO3010				
Dielectric Constant, ε_r Process	3.00 ± 0.04	3.50 ± 0.05	6.15 ± 0.15	10.2 ± 0.30	Z	-	10 GHz 23°C	IPC-TM-650 2.5.5.5 Clamped Stripline
[2] Dielectric Constant, ε_r Design	3.00	3.60	6.50	11.20	Z	-	8 GHz - 40 GHz	Differential Phase Length Method
Dissipation Factor, tan δ	0.0010	0.0015	0.0020	0.0022	Z	-	10 GHz 23°C	IPC-TM-650 2.5.5.5
Thermal Coefficient of ε_r	-3	-45	-262	-395	Z	ppm/°C	10 GHz -50 to 150°C	IPC-TM-650 2.5.5.5
Dimensional Stability	-0.06 0.07	-0.11 0.11	-0.27 -0.15	-0.35 -0.31	X Y	mm/m	COND A	IPC TM-650 2.2.4
Volume Resistivity	10^7	10^7	10^5	10^5		MΩ•cm	COND A	IPC 2.5.17.1
Surface Resistivity	10^7	10^7	10^5	10^5		MΩ	COND A	IPC 2.5.17.1
Tensile Modulus	930 823	1025 1006	1498 1293	1902 1934	X Y	MPa	23°C	ASTM D638
Moisture Absorption	0.04	0.04	0.02	0.05	-	%	D48/50	IPC-TM-650 2.6.2.1
Specific Heat	0.9		0.86	0.8		J/g/K		Calculated
Thermal Conductivity	0.50	0.50	0.79	0.95	-	W/m/K	50°C	ASTM D5470
Coefficient of Thermal Expansion	17 16 25	17 17 24	17 17 24	13 11 16	X Y Z	ppm/°C	-55 to 288°C	ASTM D3386-94
Td	500	500	500	500		°C TGA		ASTM D3850
Density	2.1	2.1	2.6	2.8		gm/cm^3	23°C	ASTM D792
Copper Peel Strength	12.7	10.2	7.1	9.4		lb/in	1 oz. EDC After Solder Float	IPC-TM-2.4.8
Flammability	V-0	V-0	V-0	V-0				UL 94
Lead Free Process Compatible	YES	YES	YES	YES				